Masters Theses   Student Theses and Dissertations

1971

Some factors affecting the results in cyclic triaxial tests

Suresh Kumar Chaudhary

SOME FACTORS AFFECTING THE

RESULTS IN CYCLIC TRIAXIAL TESTS

BY

SURESH KUMAR CHAUDHARY, 1941-

A

THESIS

Presented to the Faculty of the Graduate School of the

UNIVERSITY OF MISSOURI - ROLLA

In Partial Fulfillment of the Requirements for the Degree

MASTER OF SCIENCE IN CIVIL ENGINEERING

1971

Approved By

(Advisor)

ABSTRACT

A major cause of damage to structures and earth embank-
ments during earthquakes or any other such dynamic vibrating
loading conditions has been the liquefaction of saturated
sands. There have been several investigations to establish
a convenient and relatively simple laboratory test procedure
and to study the nature of field conditions leading to sand
liquefaction. This investigation evaluates the effects of
sample size, testing frequency, and the method of sample
preparation on the number of cycles to cause initial lique-
faction in pulsating triaxial tests using standardized
equipment and test procedures.

It has been found that sample size does affect test
results as larger diameter samples tend to give a lower
dynamic strength for sand. Also, higher pore pressures
are generated in larger diameter samples for the same
number of stress applications. There is an indication that
a higher frequency of loading also produces a lower strength,
but this is not considered to be conclusive due to very
limited data. On the other hand, it is found that the
method of sample preparation does not affect the test results
if the variables of sample preparation such as relative
density, homogenity, grainsize distribution, and the degree
of saturation are maintained reasonably constant.

ACKNOWLEDGEMENT

TABLE OF CONTENTS

LIST OF ILLUSTRATIONS

CHAPTER I

INTRODUCTION

A. General

One of the major causes of damage to structures and earth embankments during earthquakes has been the lique-faction of saturated sands. During earthquakes of Chile 1960 |6|, of Niigata, Japan 1964 |17|, and Alaska, also in 1964 |13|, extensive damage occurred due to sand lique-faction. Although similar cases of sand liquefaction were reported as far back as 1783 |12|, the recent earthquakes actually focused the attention of engineers throughout the world on the importance of this phenomenon and its devas-tating effects.

Apart from the importance of liquefaction of saturated sand during earthquakes, the changing requirements of tech-nology and society at large, as well as the world political situation, have created potential or actual conditions where the danger of sand liquefaction substantially exists. Present design should consider shocks caused by large nuclear or conventional blasts for earth excavation or potential wartime explosions which generate a wave front of great peak stress. Radar or electrical transmission tower vibrations due to wind and foundations of unbalanced machinery may cause less spectacular failures. The latter type of vibrations are of small amplitude, but they occur for a great many cycles and are similar to earthquake conditions |11|.

The cause of liquefaction of saturated sands has been understood qualitatively for many years. If a loose saturated sand is subjected to vibrations, it tends to compact and decrease in volume; if drainage cannot occur, the tendency for the volume decrease results in an increase in pore-water pressure. Thus, if the pore-water pressure builds to a magnitude where it equals the over-burden pressure, the effective stress is reduced to zero with the consequent loss of sand strength. This is liquefaction.

The liquefaction of saturated sand may develop in any zone of a soil deposit where the necessary combination of in-situ conditions and vibratory excitation occurs. Such zones may be at the surface or at some depth below the ground surface depending only on the state of the sand and the induced motions |23|.

Most of the earlier investigations have sought to establish a simple procedure to simulate liquefaction in the laboratory to facilitate a comprehensive study of liquefaction potential of sands. This would help predict the susceptibility of sand deposits to liquefaction and, thereby, development of design criteria.

B. Scope of This Investigation

There have been several investigations on the lique-faction phenomenon of saturated sands. Lee |13|, Lee and Seed |14|, and Seed and Lee |23|, at the University of California have extensively studied liquefaction of sands and, at the same time, developed a new concept of instru-

mentation which closely simulates the dynamic loading
conditions in the field |23|. Subsequently, Rocker |20|
investigated sand liquefaction using Seed's and Lee's con-
cepts but with different materials and equipment.

On the other hand, Castro |3| carried out investiga-
tions in which the approach was monotonic loading. He
attempted to determine and establish the validity of
earlier concepts of critical void ratio by Casagrande |4|,
as applied to the liquefaction of saturated sands.

Although these investigations corroborated the basic
assumptions and the underlying concepts postulated by Seed
and Lee |23|, there is one striking difference in all
these investigations. They were carried out on different
materials, with different equipment configurations, using
different sizes and methods of sample preparation, and
using different frequencies of cyclic loading. Without
knowing the effects of these variables, it is difficult
to compare the results. It is doubtful that direct com-
parisons can be made |25|. No standardized equipment and
procedures exist for the dynamic soil test.

It is the purpose of this investigation to document
test procedures and equipment and evaluate the effects of
sample size, testing frequency and method of sample prep-
aration on the number of cycles to cause initial lique-
faction in triaxial samples.

CHAPTER II

LITERATURE REVIEW

A. Previous Studies

Probably the first attempt to delineate conditions
under which liquefaction might occur is the critical void
ratio approach suggested by A. Casagrande |4|. It was
noted that during shear, dense sands tend to expand whereas
loose sands tend to decrease in volume. Thus, for any sand
there must be some void ratio, for which there is no volume
change at failure. This void ratio is called the critical
void ratio. It was reasoned, therefore, that sand deposits
having a void ratio higher than the critical void ratio
value will tend to contract during shear. Under undrained
conditions, they would develop positive pore-water pressures
which might possibly become large enough to reduce the effec-
tive overburden and confining stresses to zero, thereby
reducing the shear strength to zero. This produces lique-
faction. Conversely, deposits having a void ratio lower
than critical would tend to increase in volume, causing a
negative pore-water pressure under the undrained shear con-
ditions. A higher effective stress is developed in the soil
mass, increasing the strength and stability.

Subsequent to Casagrande's work, it has been noted
that the critical void ratio is not a constant value for
a given sand, but depends on the confining pressure to
which the sand is subjected |54|. Because dilation ten-

dencies are smaller at high confining pressures, the critical void ratio decreases as the confining pressure increases. It has been concluded that a saturated sand at a given density is potentially less stable under high confining pressures than under a low confining pressure. This approach can provide a valuable guide to the behavior of saturated sands subjected to loading. However, as Casagrande noted |4| in presenting the concept of critical void ratio, volume change under cyclic loading conditions are quite different from those occurring under one-dimensional static loading conditions. It could hardly be expected that the critical void ratio concept would be applicable to earthquakes or vibratory loading conditions. In fact, Russian engineers have noted the "breakdown" of sand structure below the critical void ratio and, on the contrary, the satisfactory behavior of many structures built on sand with a void ratio above critical |16|.

The inadequacy of the critical void ratio approach for vibratory loading problems has led engineers to attempt to establish the conditions producing liquefaction in terms of the acceleration at which liquefaction can be observed to develop |16,19|. Usually the testing is done by placing saturated sand in a box on a shaking table and recording the table acceleration at which the liquefaction occurs. Such results, however, are inevitably influenced by the duration and frequency of the table motion to which the sand is subjected and possibly also by the geometry

and the deformation characteristic of the container. Thus,
it is very difficult to extrapolate the test results to
field conditions |23|.

In the period of 1937-39, J.D. Watson |24| conducted
a comprehensive study on the representative sand samples
from hydraulically deposited shells of the Fort Peck Dam.
These and other investigations on the sands from the
Fort Peck Dam indicated that the critical void ratio as
determined from laboratory tests was higher than the void
ratio of the sand in the Dam; on this basis, liquefaction
could not have occurred. However, Casagrande explained
in his lectures on Soil Mechanics at Harvard |3| that his
investigations on the Fort Peck Dam failure led to two con-
clusions. First, that the sands in the shell and the
foundation of the Dam had indeed experienced a major lique-
faction failre; and secondly, that the method used for
determining critical void ratio was faulty and led to
erroneous results. Largely as a result of his investigation
of the Fort Peck Dam slide, Casagrande developed the concept
of the "flow structure" |24|, which he described in his
lectures. He assumed that during a liquefaction slide,
the relative position of the grains is constantly changing
in a manner which maintains a minimum resistance. The
change from a normal structural arrangement of the grains
to the "flow structure" would start almost accidentally in
a nucleus and then spread through the mass by a chain re-
action; and that such a reaction could explain the spon-

taneous character of liquefaction. With the failure of
several efforts to investigate liquefaction in the
laboratory, he thought that it might never be possible to
reproduce on small test specimens the conditions which
produce liquefaction in an element within a large mass of
saturated sand |24|.

In 1958, Roscoe |22| reported a series of consolidated-
drained tests on cohesionless materials, performed with a
simple shear device that he had developed earlier |21|.
He found a better agreement with critical void ratio
concept on the final void ratios on steel balls and glass
beads than on sands. He attributed the difference, to a
certain extent, to the particle breakdown suffered by sands
during the tests.

B. Effects of Vibration on Saturated Sand

Up to this point, references have been made to inves-
tigations of the critical void ratio concept, which is
applicable to the behavior of a sand when subjected to large
monotonically increasing shear deformation. It has been
observed that liquefaction failures are also induced by
cyclic strains caused by earthquakes and vibratory conditions
developed in structures. As mentioned earlier, when a
strong vibratory disturbance acts on a loose sand mass,
it tends to produce a reduction in volume. The volume
decrease tendency produces a cumulative rise in pore-water
pressure. Maslov |16|, Florin et. al. |9|, Barkan |1|,

Bazant et. al. |2| have reported results of investigations in which the variables affecting this rise in pore-water pressure have been studied.

Nunnally published results on four saturated sands in 1966 |18|. The tests were similar to those of Maslov, and he found that the magnitude of pore-water pressure developed during vibration could be related to the grainsize characteristics of the sand.

A comprehensive study of the effects of controlled cyclic stresses on the deformation of sand samples and the pore-pressure build-up has been carried out by Lee |13|, Lee and Seed |14|, and Seed and Lee |23|. The materials used in these investigations consisted of a clean uniform sand from the Sacramento river in California. The sand specimens were loaded in a triaxial apparatus modified to allow the cycling of deviator stress. The frequency of loading ranged from 2 Hz to 5 Hz, but mostly 2 Hz. The cyclic loading pattern was a square wave shape. In these tests, the cycled deviator stress termed σ_{dp}, the pore water pressure and the axial deformations were recorded. A typical result is given in Figure 2.1.

They concluded that negligible axial strains occur in loose sand until the pore-pressure builds up to equal the effective confining pressure. This reduction of effective stress to zero is defined as liquefaction. For dense sands, the pore-pressure gradually increases with each successive cycle. The sample deformation increases with each cycle,

Test No 114
initial void ratio = 0.87
initial confining pressure = 2.0 kg per sq cm

(a) TYPICAL PULSATING LOAD TEST
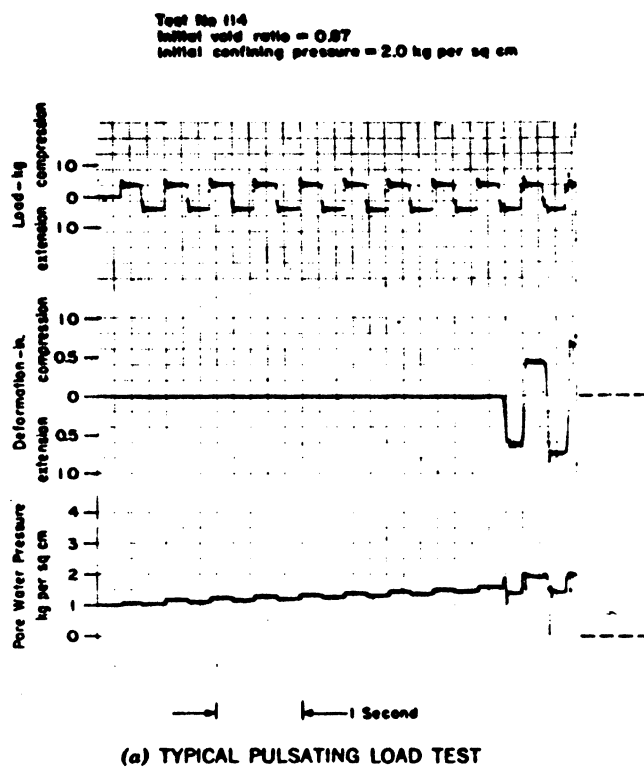
Fig. 2.1   Reversing Stress Test on Loose Sand
Seed and Lee |23|.

but the axial strain is small until the maximum value of σ_3'/σ_1' in extension is reached. Thereafter, the axial strain increases markedly with each subsequent cycle.

Seed and Lee |23| suggest that the following conditions may be recognized in cyclic triaxial tests:

1. Failure is when strains become excessive. Therefore, the failure of a sample depends on the definition of the failure criteria adopted for the tests. In their tests, it is usually defined as 20% axial strain, double amplitude, or a ±10% axial strain.

2. Complete liquefaction is when the soil exhibits negligible or no resistance to deformation over a wide range of strain.

3. Partial liquefaction is when a soil offers no resistance to deformation over a range of strain less than failure strain.

4. Initial liquefaction occurs when the soil exhibits any degree of partial liquefaction, i.e. when the pore-pressure first equals the effective confining pressure.

Based upon the above criteria, Seed and Lee |23| derived the following conclusions:

Cyclic stress application will induce partial liquefaction over a wide range of relative densities. The magnitude of cyclic deviator stress to cause liquefaction is a given number of cycles increases with increasing relative density or decreasing void ratio.

A higher effective confining stress requires a greater cyclic deviator stress to cause liquefaction for the same number of cycles.

The larger the cyclic stress or strain, the lower the number of cycles required to cause liquefaction.

For loose sands, the initial liquefaction, excessive strain, and complete liquefaction occur simultaneously. For denser samples, the magnitude of cyclic deviator stress and number of cycles to failure are related to the failure criterion adopted.

One other aspect of the cyclic test was also noted by Seed and Lee |23|. A difference in behavior of the sand occurs when samples are cycled in compression only, as opposed to when cycling is done with stress reversal. Stress reversal is defined as a change in deviator stress from compression to extension passing through zero deviator stress. In this manner of cyclic loading, the lateral confining stress becomes the major principal stress on the upward or extension stroke. On the basis of observations of such reversing stress tests, Seed and Lee concluded:

A dense sand under low consolidation stress was noticeably weaker in reversing stress loading than under non-reversing conditions.

The effect of strength reduction due to stress reversal is greatly reduced for loose sands, and for samples under higher confining stresses.

In all cases, cyclic loading induced axial strains

which increased with continuing cycles.

The specimen strength under cyclic loading increases with increasing density and with increasing confining pressure.

The greater the consolidation ratio, $\sigma'_{1c}/\sigma'_{3c}$, the greater is the deviator stress required to cause failure for samples undergoing stress reversal.

Peacock and Seed [19] reported results of cyclic simple shear tests on saturated Monterey sand. The behavior in cyclic simple shear was similar to the triaxial behavior but there was a considerable discrepancy in the magnitude of stresses to cause failure in the two different tests. The cyclic simple shear stress required to cause liquefaction failure is approximately 35% of the stress determined in triaxial tests. However, this figure has been increased to 50 to 65% [19].

Lee and Fitton [15] performed a series of cyclic triaxial tests to determine the effect of grain size, grain size distribution and grain shape on the strength of the soil under cyclic loading. The testing procedure was similar to that of Seed and Lee [23]. They concluded that D_{50}, the median soil particle diameter, presented a reasonably satisfactory basis of comparing the dynamic strength of one soil to that of another. The cyclic deviator stress to cause failure was found to be dependent on the mean grain size. As the mean grain size decreased, they also concluded that grain size distribution and grain shape were

considerably less significant than the grain size. They further observed that there can be variation in the result due to the size of the specimen, but they did not consider it important |15|.

Castro |3| performed a series of tests in which he tried to explain "spontaneous liquefaction". He defined liquefaction as that particular phenomenon which takes place in a mass of sand during flow slides. This flow, which he termed as "liquefaction", is caused by a large reduction in the shear strength of soil. A loose saturated sand reaches its ultimate shear resistance at small strains in undrained cyclic stress reversal tests. Further straining induces a large reduction in shearing resistance. This reduction in shear resistance is a manifestation of the tendency of the sand structure to decrease in volume, which in turn results in an increase of pore-pressure. Castro concluded from the tests that the rapid large shear strain induces a change in the sand structure until it reaches a "minimum resistance structure", when the flow takes place. In his opinion, the shear strength during such a flow is a function of the void ratio of a particular sand and also of its grain size distribution.

Castro applies this flow structure concept also to cyclic loading conditions. He theorizes that loose sand will fail suddenly if the pore pressure is increased by any agency. The shear strength then decreases below that required for stability. The sand will shear continuously

at a reduced shear strength until it comes into equilibrium under a reduced resistance. The strength during flow will be governed by the void ratio, provided no drainage occurs. If the effective confining pressure during flow is known, the resistance to flow can be calculated. The plot of effective confining pressure $(\bar{\sigma}_{3f})$ during flow on a log scale versus the void ratio falls on a slightly curved line, which he called the e_f-line. The effective confining pressure under which the samples deformed with constant resistance is the same as that computed from the e_f-line previously determined by the drained static tests.

The e_f-line concept proposed by Castro is akin to the critical void ratio concept which was earlier put forward by Casagrande |4| for static conditions; Castro has tried to apply it to the dynamics. It is not clear from his investigation what is the effect of strain rate on the strength of sand. The determination of susceptibility of sand deposits to liquefaction by this method is open to question. The shear resistance during a flow may be computed and can be presented by the e_f-line. However, this does not take into account the increase in vibration or cyclic shear stress necessary to cause a flow condition with an increase in confining pressure. On the contrary, he suggests that the greater the confining pressure, the greater would be the loss in strength, and the sand will be more susceptible to liquefaction.

Liquefaction, as defined by Castro, is not the same as

defined by Seed and Lee |23| and other investigators. The
definition used by Castro applies to the shear resistance
of sands during flow slides caused by an increase in pore-
pressure due to overstressing of sand or by any other reason.
This phenomenon is often termed as "spontaneous liquefaction"
when sand flows until it stabilizes under the reduced
strength.

At best, this method estimates the strength of soil
during rapid deformations but not the loss of strength
under vibration itself. Therefore, it can be used as an
adjunct to the other tests, which can predict the number of
cycles for a particular condition for causing liquefaction
in saturated sand. Castro's method can estimate the resis-
tance of the liquefied soil, once it has started straining.

Rocker |20| reported a series of investigations
similar to those of Seed and Lee |23| on a clean uniform
natural sand and on a modified natural sand. A sample 2.8
inches in diameter was used. The tests generally correlated
well with Seed and Lee |23| but the strength was low com-
pared to the earlier tests of Seed and Lee |23| on a similar
sand. Rocker attributed this to the rounded grain shape
of the sand used in his investigation |20|.

Finn et.al. |8| have reported the effects of previous
strain history on the liquefaction potential of sand.
According to their investigations, if the sand has strained
previously and has suffered liquifaction, it is more
susceptible to liquefaction afterwards than a soil which

has not been liquefied in its history. Samples, stabilized after liquefaction in dynamic triaxial tests, reliquefied at a considerably less deviator stress and number of cycles. This phenomenon occurred in spite of the increase in relative density due to volume changes which took place during the dissipation of excess pore-pressure stabilizing the sample after liquefaction.

CHAPTER III

MATERIAL

The sand used in this investigation was obtained from the Lane Spring Recreation Area on the Little Piney River in Phelps County, Missouri. It is uniformly graded medium to fine sand, with a Unified Soil Classification symbol of SP. Figure 3.1 presents the grain size distribution curve for this material.

The physical properties of the sand are given in Table I. The specific gravity of the material was determined by the ASTM test procedures based on an average of four tests. The determination of maximum relative density was carried out in two different ways and the higher of the two values was accepted as the maximum relative density |10|.

TABLE I

PHYSICAL PROPERTIES OF LANE SPRING SAND

Specific Gravity............................ 2.64

Minimum Void Ratio......................... 0.487

Maximum Void Ratio......................... 0.751

Minimum Dry Density........................ 93.9 lb/cu.ft.

Maximum Dry Density........................ 110.7 lb/cu.ft.

Grain Size Distribution

      Coefficient of Uniformity, Cu.......... 1.6

      Coefficient of Curvature, Cc........... 1.1

Unified Classification..................... SP
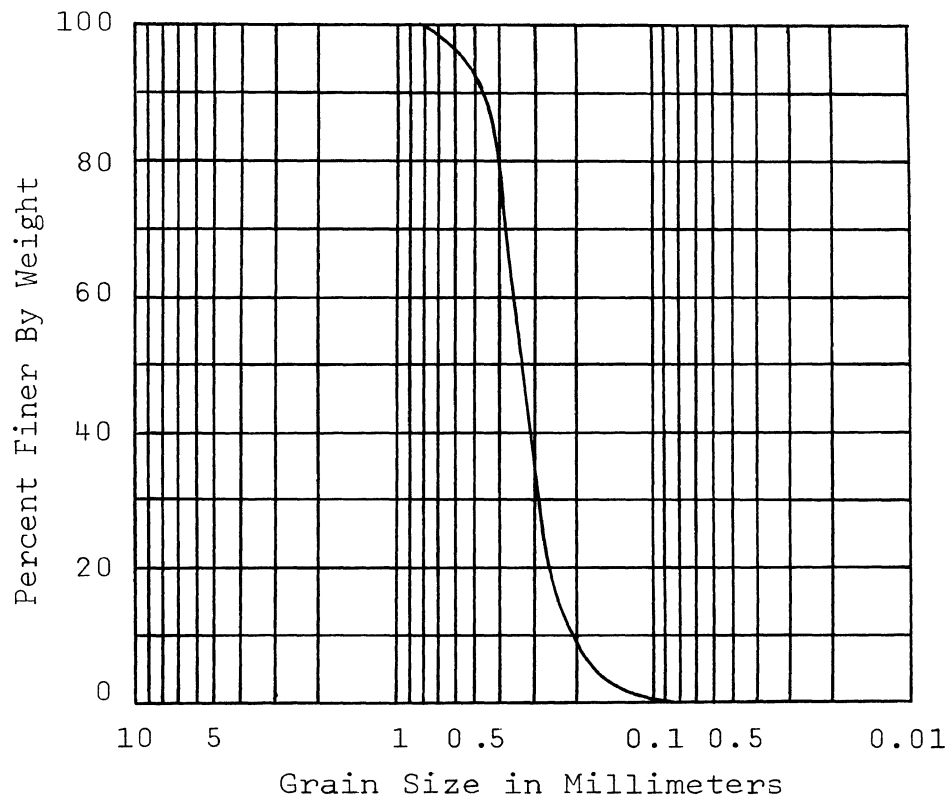
Lane Spring Sand
Source: Lane Spring Recreation Area
Little Piney River
Phelps County, Missouri

Fig. 3.1   Grain Size Distribution Curve
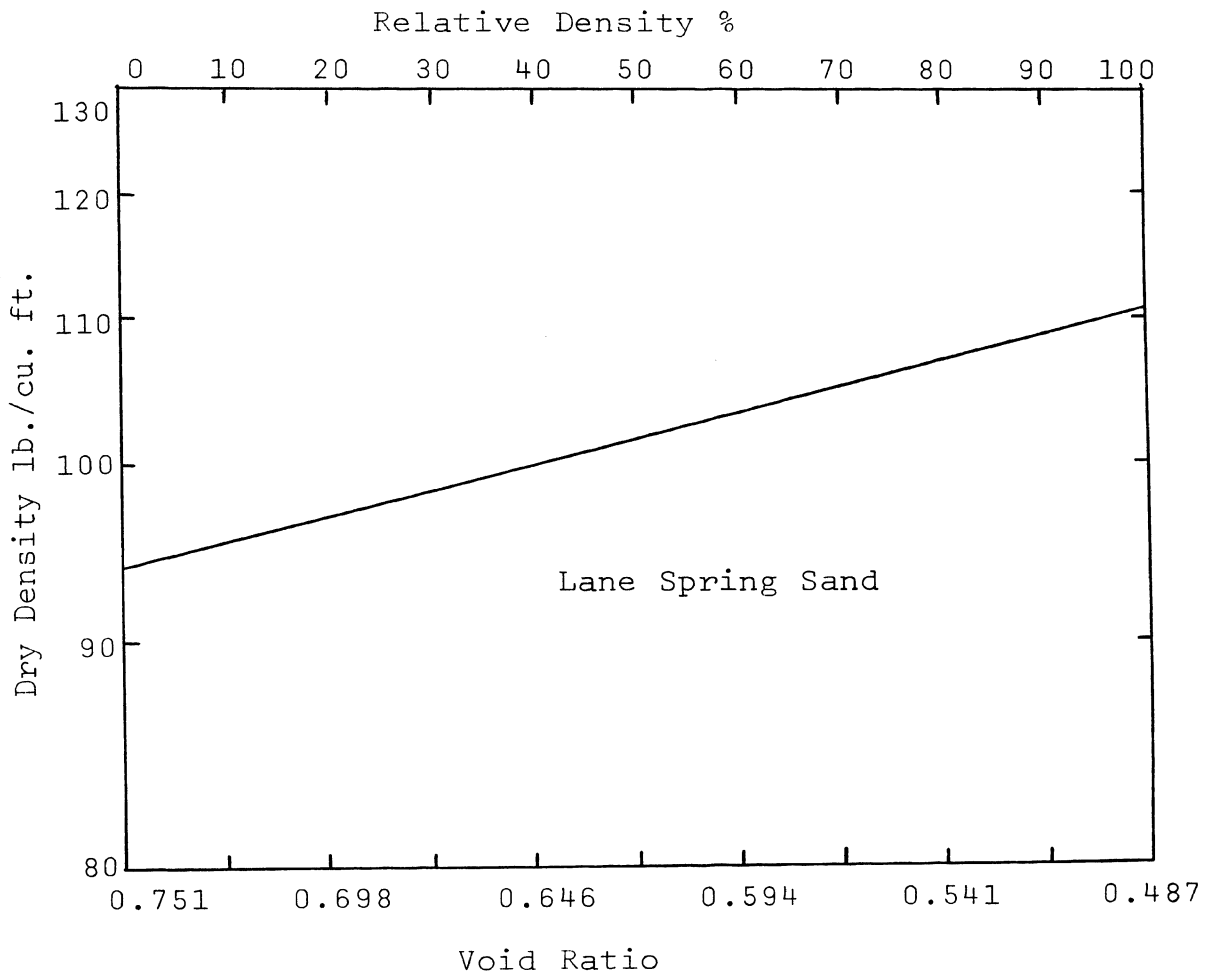
Relative Density %

Fig. 3.2 Relationship Between
Dry Density and Relative Density
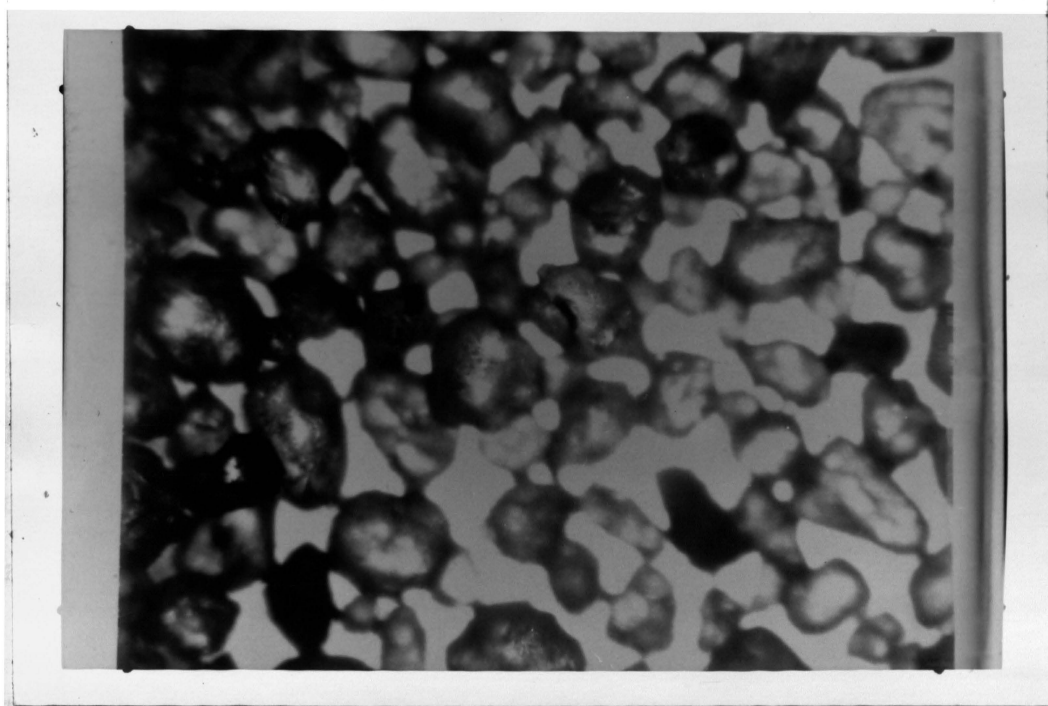
Fig. 3.3 Photomicrograph

Magnification 40 X

CHAPTER IV

EQUIPMENT AND TEST PROCEDURES

A. Equipment

The equipment shown schematically in Figure 4.1 consists of a triaxial chamber, a double acting piston, and a control unit. The triaxial cell has an interchangeable platen capability for testing specimen sizes of 1.4", 2.8", and 4.0" in diameter. The double acting piston provides cyclic stress-controlled loading and the control unit is equipped to regulate chamber pressure, back pressure, cyclic deviator stress, and the frequency of loading. An electrical counter automatically records the number of stress cycles.

In addition to the above main components, the system is also equipped with several electrical sensors to facilitate measurements of axial load, deflection, and pore-pressure.

A strain gage load cell is placed rigidly between the double acting piston and the loading cap of the specimen, and is located outside the triaxial chamber. See Figure 4.3.

The pore-pressure responses are monitored by a VIATRAN strain gage pressure transducer, mounted outside the triaxial cell. See Figure 4.4.

The deformation of the sample is measured by a HEWLETT-PACKARD, D.C. Linear Variable Differential Transformer mounted on top of the triaxial cell and attached
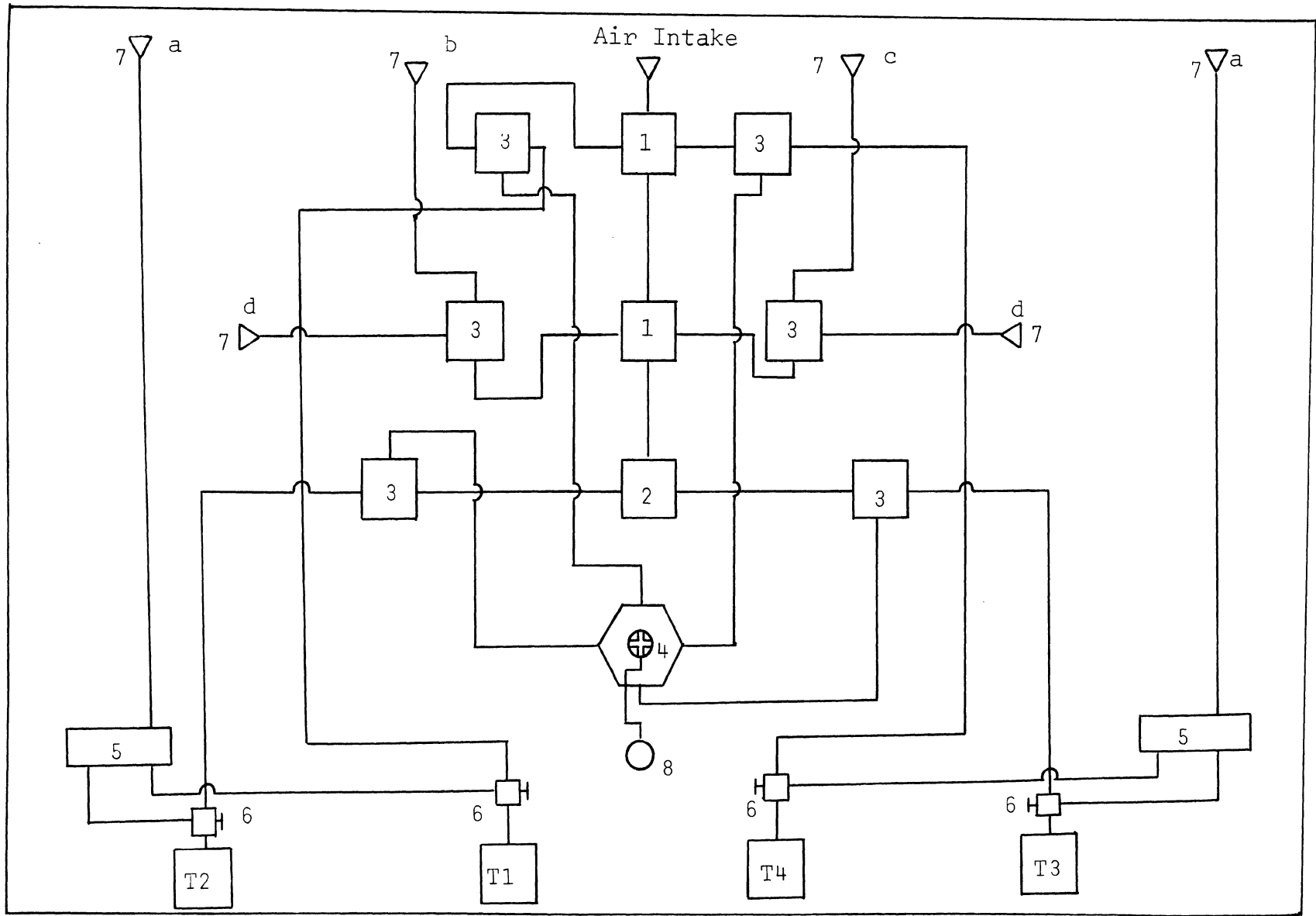
Fig. 4.1   Schematic Diagram of Air Pressure System of Cycle Control Panel for Dynamic Triaxial

TABLE II

Key to Figure 4.1

1. Four-way Swagelock Junction.

2. Three-way Swagelock Junction.

3. 0 - 15 PSIG Fairchild Pressure Regulators.

4. Distributor Manifold with Pressure Gage.

5. Electrical Solenoid Valves.

6. Air Bleed Valves.

7. Pressure Outlets

    a. Inlet-Outlet to Double Acting Piston.

    b. To Chamber Pressure.

    c. To Back Pressure.

    d. Chamber and Back Pressure Gages.
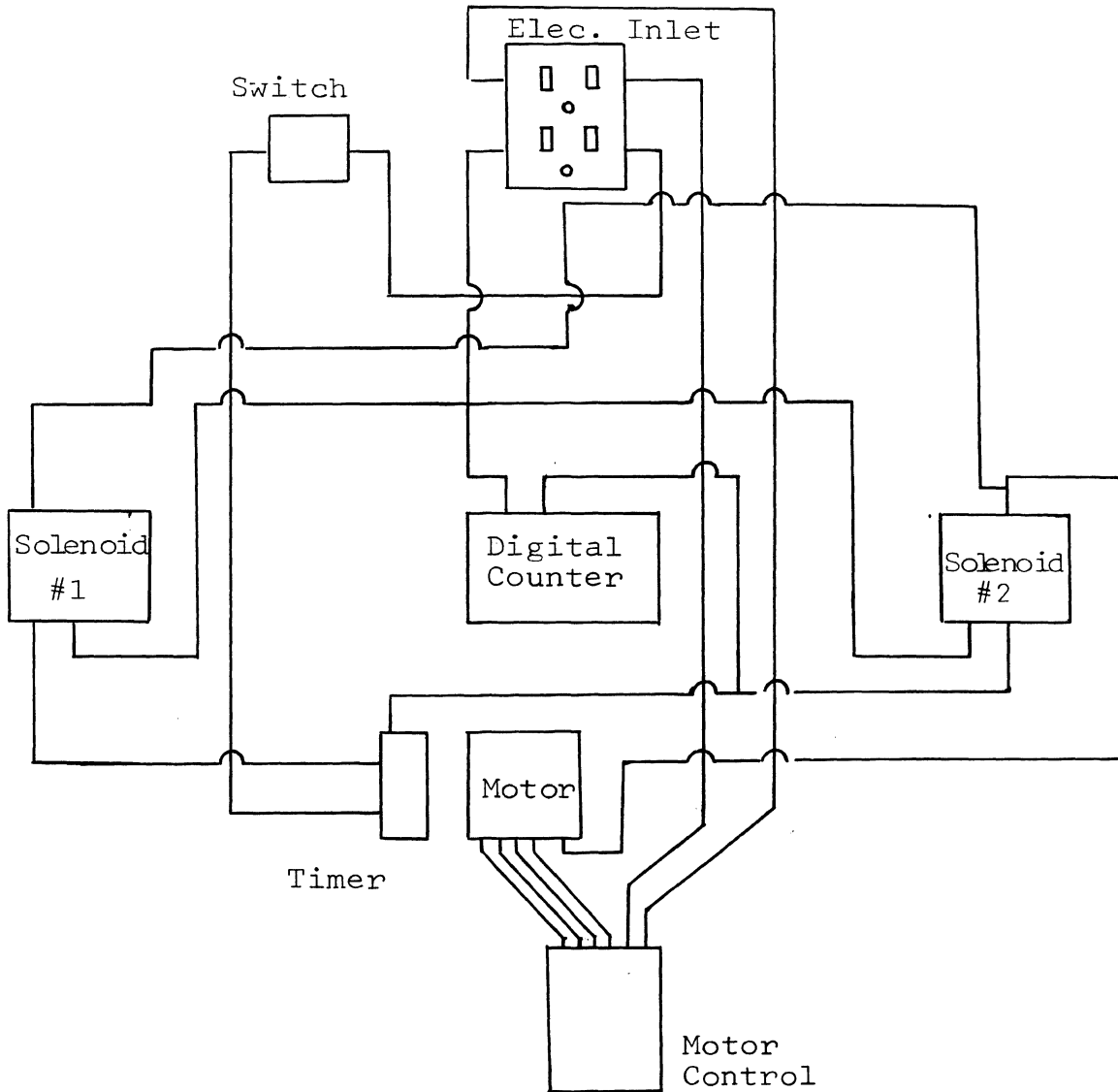
Fig. 4.2 Electrical Circuit Diagram
of Cyclic Triaxial Panel
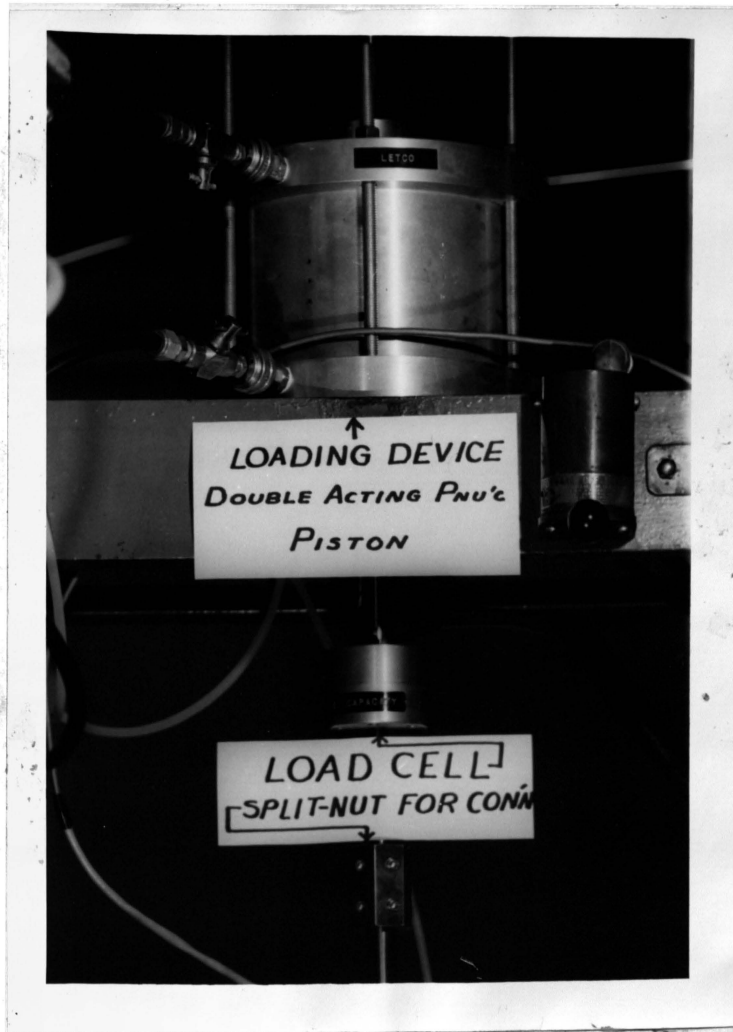
Fig. 4.3   Arrangement of Load Cell
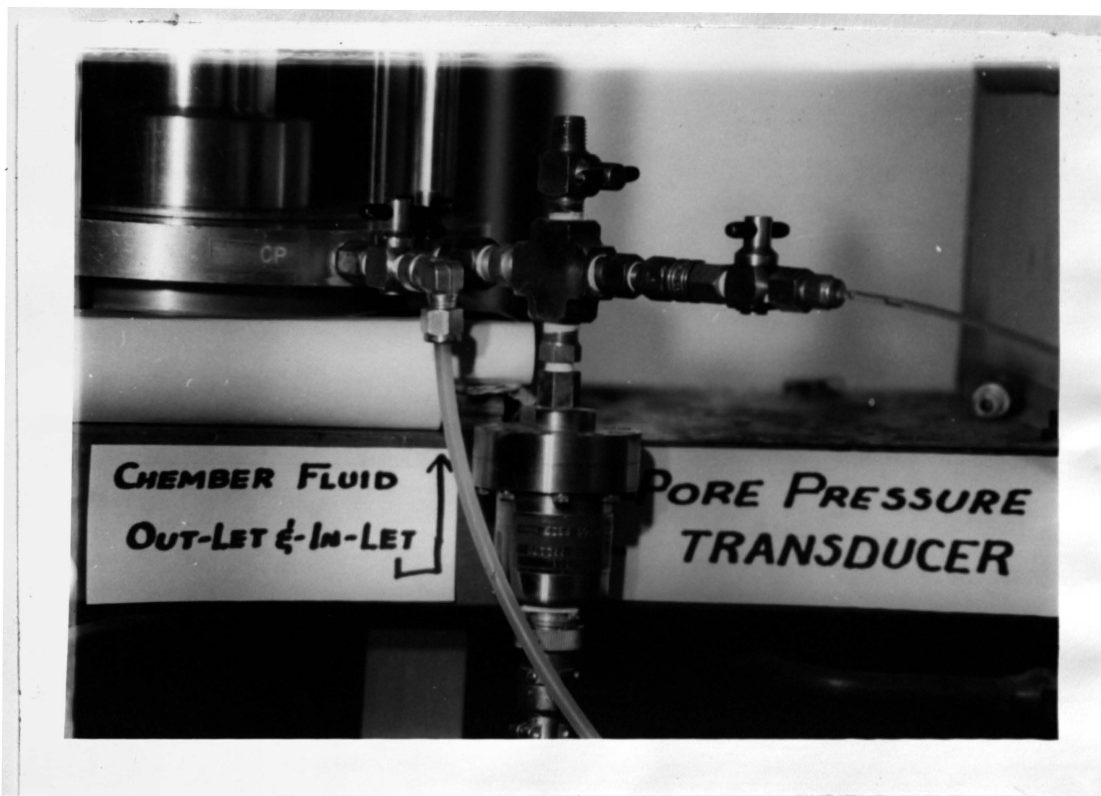
Fig. 4.4 Arrangement of Pore-Pressure Transducer

Fig. 4.5 Arrangement of LVDT for
Deformation Measurement
(Note the Unattached Piston)

(Photo Taken for Demonstration Purposes)

to the piston rod. A typical arrangement for the triaxial test is shown in Figure 4.5.

The electrical signals from the load cell, pore-pressure transducer, and the LVDT are recorded on a Honeywell multichannel light beam oscillograph.

The chamber and back pressure are applied through water by compressed air; also compressed air is cycled to the double acting piston by electrically controlled solenoid valves. A Minerah speed control device is used to vary the test frequencies from static loading to 10 Hz.

A detailed description of equipment is given in Appendix IV.

B. Specimen Preparation

To investigate the effects of variations of specimen preparation methods on the test results, samples were prepared in three different ways corresponding to methods used by previous investigators.

Since the initial void ratio, saturation, and homogenity of the specimen are of the utmost importance, it was necessary to establish a suitable method of preparation in which these variables would not be responsible for variation in test results. Three methods of sample preparation were tried. A more detailed description is given in Appendix C.

Method "A" -- A predetermined amount of sand to achieve a particular density is boiled under vacuum to remove air entrapped between the sand grains. After cooling, the sand

the sand is introduced into a submerged specimen mold,
the operator taking care to use deaired water and not
letting the sand become exposed to the atmosphere.

Method "B" -- The specimen is formed with dry sand
to the required density and deaired water is introduced into
the bottom of the specimen by back pressure. The water
level is slowly raised inside the sample.

Method "C" -- This method of preparation is somewhat
similar to the method "A", but instead of preparing the
sample under water, the specimen mold is prefilled with
water, and dry sand is introduced into the mold in layers.
A certain depth of free water is always maintained on top
of the sand, until the cap is placed on top of the formed
sample.

Method "A" produces the best and most reproducible
sample as far as the ease of saturation is concerned. The
other methods are used to compare the effects of sample
preparation on test results.

C. Test Procedure

After selection of the relative density, effective
isotropic consolidation pressure, and the specimen size,
the sample is formed by one of the sample preparation
methods outlined. All of the samples are formed in a
thin commercial rubber membrane, attached to the base of
the mold by a rubber band. Several additional membranes
are placed over the specimen to insure that the single
membrane will not rupture during the test. The triaxial

cell is assembled and filled with water as the confining
fluid. The sample is checked for 100% saturation by deter-
mining the value of Skempton's pore-pressure coefficient B.
Necessary back pressure is applied in small increments to
achieve 100% saturation. The value of B, equivalent to
100% saturation, was found to be 0.98, based on experimental
verification.

When the saturation is considered to be 100% or very
nearly 100%, the drainage line is opened, the cell pressure is
increased to the required level of consolidation pressure,
and the sample is allowed to consolidate. To achieve an
isotropic consolidation condition, the piston rod is not
attached to the sample cap at this time, as shown in
Figure 4.5. After consolidation is complete, the piston rod
is then rigidly attached to the sample; but in order to
compensate for piston uplift, it is necessary to apply a
downward force on the double acting piston to counterbalance
the uplift. The counterbalancing downward force is always
determined experimentally in this investigation.

At this point, it is important to understand the
working of the double acting piston. The double acting
piston is a small air-tight chamber, six inches high by
six inches in diameter, divided in the middle by two
flexible diaphragms; both the upper and the lower chambers
are provided with one inlet-outlet orifice connected to
the air supply. The device has two strokes--upward and
downward--depending on the direction of the pressure

differential. When the upper chamber is filled with compressed air, the diaphragm moves downward and exerts a force proportional to the air pressure on the piston rod; at this moment, when the upper chamber is under pressure, the lower chamber is connected to a cylinder at atmospheric pressure. This facilitates bleeding the lower chamber as the diaphragm moves downward. With the activation of the solenoid valve for the upward stroke, the upper chamber is opened to exhaust, while the lower chamber is filled with compressed air thereby inducing an upward force in the piston rod. Since there are only two orifices in the piston chamber, when the push load acting downward is connected to the upper chamber, the lower chamber orifice (pull exhaust) is connected to the atmospheric chamber, the upper chamber automatically goes to the exhaust setting (push exhaust). In this equipment, push load and pull exhaust and pull load and push exhaust work simultaneously.

Before the specimen is cycled, the drainage connection is closed, the cycle counter reset to zero, and the recorder turned on. The choice of recording paper speed depends on the estimated time of the test and also on the frequency of loading.

A typical test recording is shown in Figure 4.6 where axial load, pore-pressure and displacements are recorded at constant paper speed.
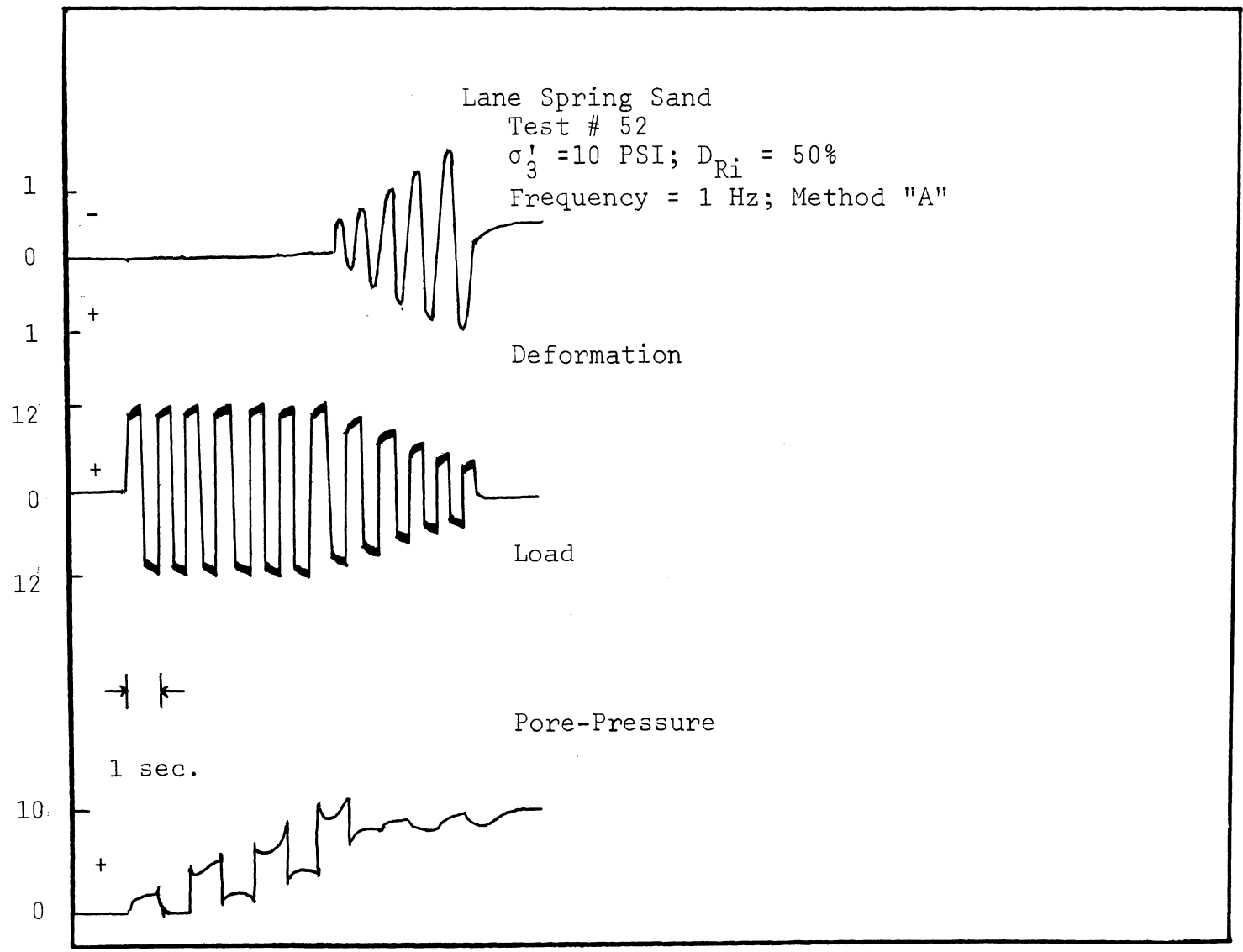
Fig. 4.6   Reproduction of the Typical Output-Reversing Stress Test Data From Honeywell Light Beam Recorder

CHAPTER V

PRESENTATION OF RESULTS AND DISCUSSION

A. Test Results

The results of this investigation have been set forth
in the form of graphs, Figures 5.1 through 5.11. In all
instances, the deviator stress has been normalized by
dividing it by the effective confining stress. Similarly
the pore-pressures are normalized by dividing the pore-
pressure at any particular time by the effective confining
stress. The cycle of pore-pressure is normalized by
dividing it by the number of cycles causing initial lique-
faction.

Figure 5.1 presents the results of what has been
termed as a standard test: a test on a sample 1.4" diameter
and 3.2" high with a relative density of 65%, a loading
frequency 1 Hz, an effective confining pressure of 10 PSI,
and prepared by method "A". It also shows the results of
tests on similar samples with relative densities of 50%
and 80% with other variables held constant. For this
graph, the normalized deviator stress is plotted against
the number of loading cycles required to induce the initial
liquefaction in the samples.

Figure 5.2 depicts the results of tests on a standard
sample with a loading frequency of 2 Hz.

Figure 5.3 shows the results of tests similar to the
standard tests as presented in Figure 5.1, but with a 2.8"
diameter, and 6.98" high sample. The results of tests at
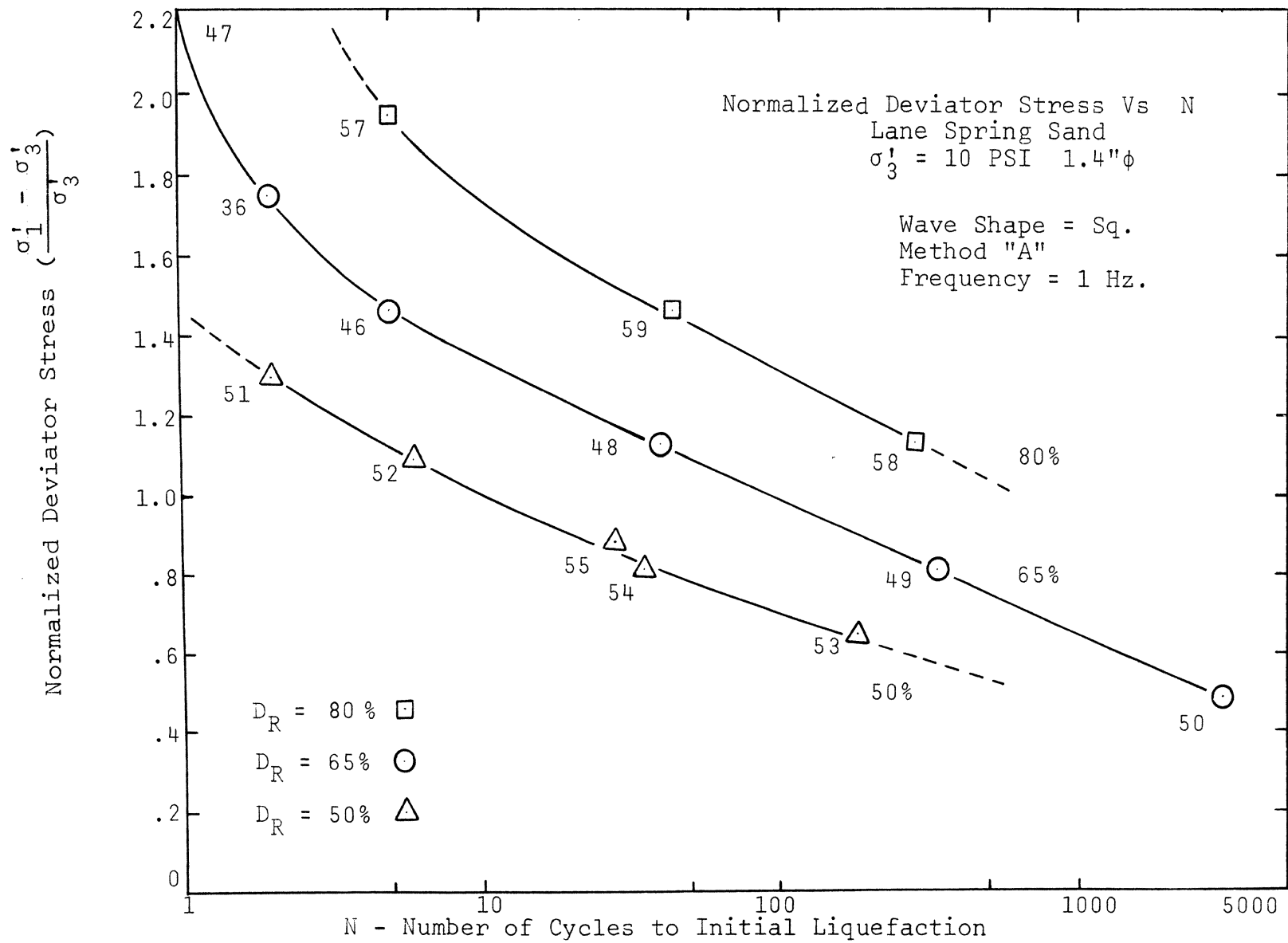
Fig. 5.1   Test Results of Reversing Stress Tests on 1.4" Diameter Sample

35
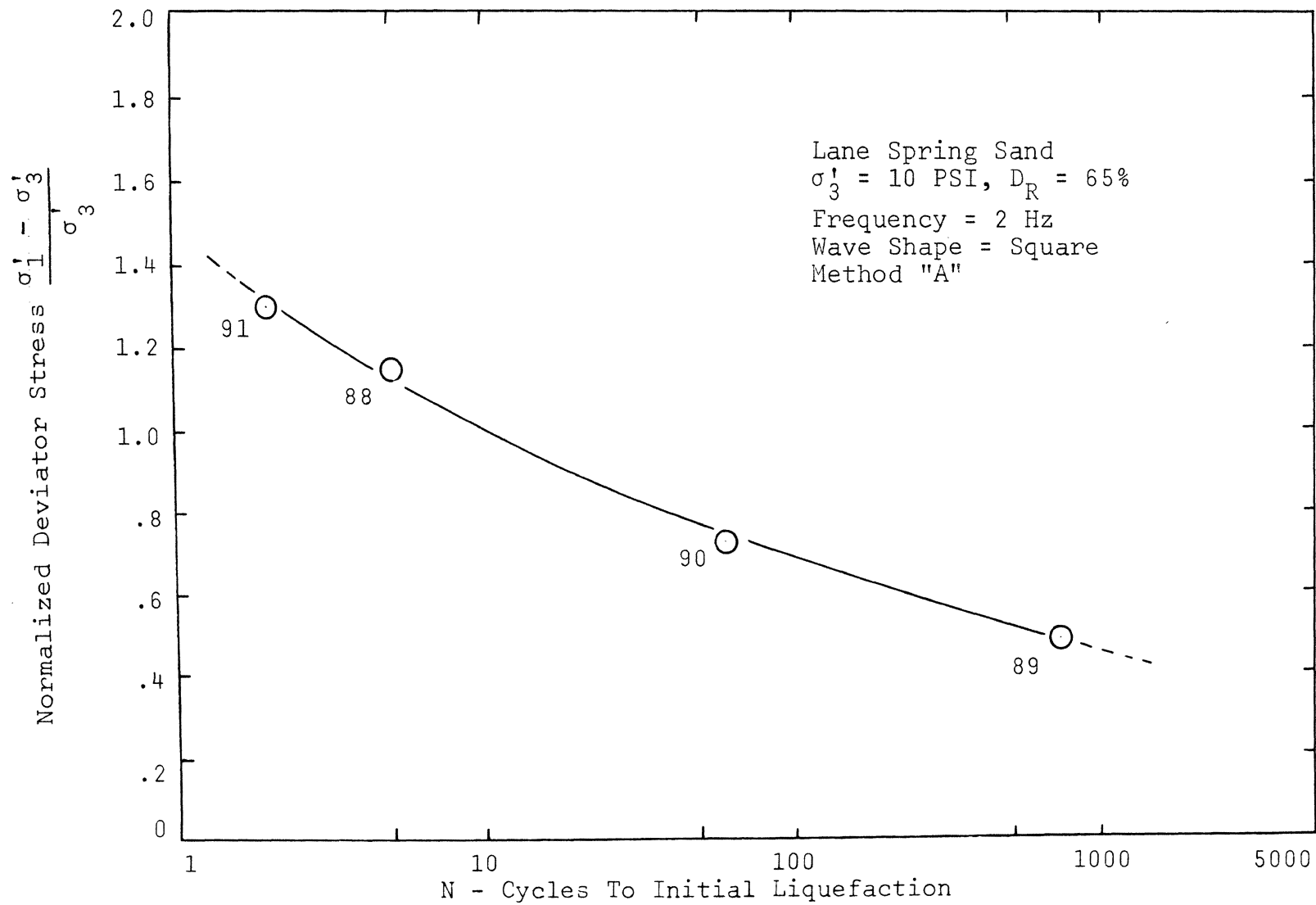
Fig. 5.2 Test Results of Reversing Stress Tests on Standard Samples with the Frequency of 2 Hz.
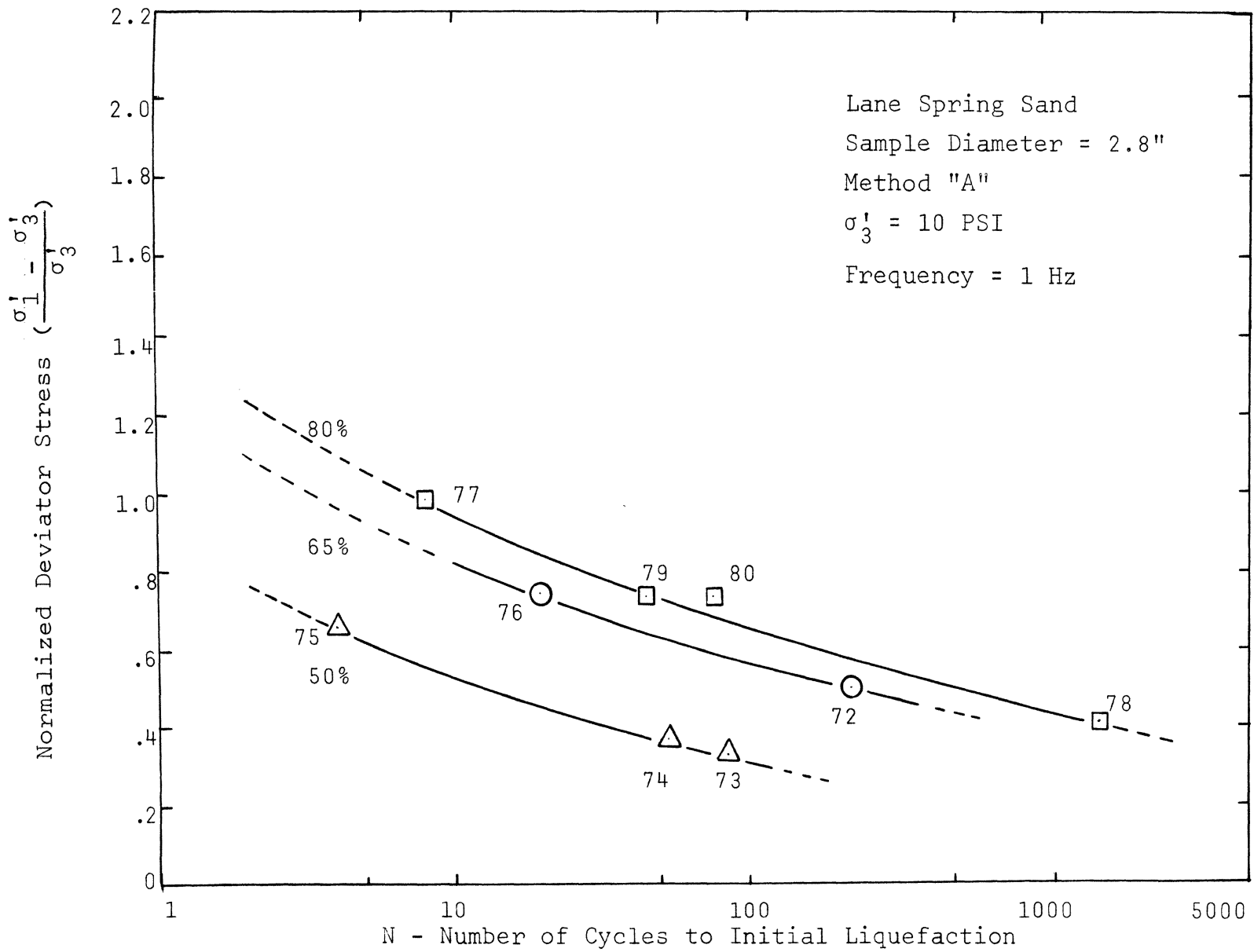
Fig. 5.3 Test Results of Reversing Stress Tests on 2.8" Diameter Samples.

50% and 80% relative density on this size sample are also
plotted on the same graph. Figure 5.4 presents test results
of 4" x 8" samples, and also summarizes the results of
1.4", 2.8" and 4.0" diameter samples with a relative
density of 65%.

Figures 5.6 and 5.7 present the relationship of sample
size to the normalized deviator stress required to cause
initial liquefaction in a particular cycle.

Figure 5.8 is a summary of results of the pore pressure
responses of the three different sample sizes. The plot of
normalized pore-pressure response versus the normalized
cycle of failure depicts the state of pore pressure build-
up within samples of different sizes at any particular time
during the test.

Figure 5.9 shows the relationship of relative density,
both initial and after consolidation, and the normalized
deviator stress required to cause initial liquefaction.

Figure 5.10 shows the relative density produced by an
effective confining stress of 10 PSI on samples of
different sizes prepared at different initial relative
densities.

In Figure 5.11, the dynamic response of sample method
"C" is compared with the standard test on 1.4" diameter
samples. There is obviously no effect of sample preparation
method on the test results.
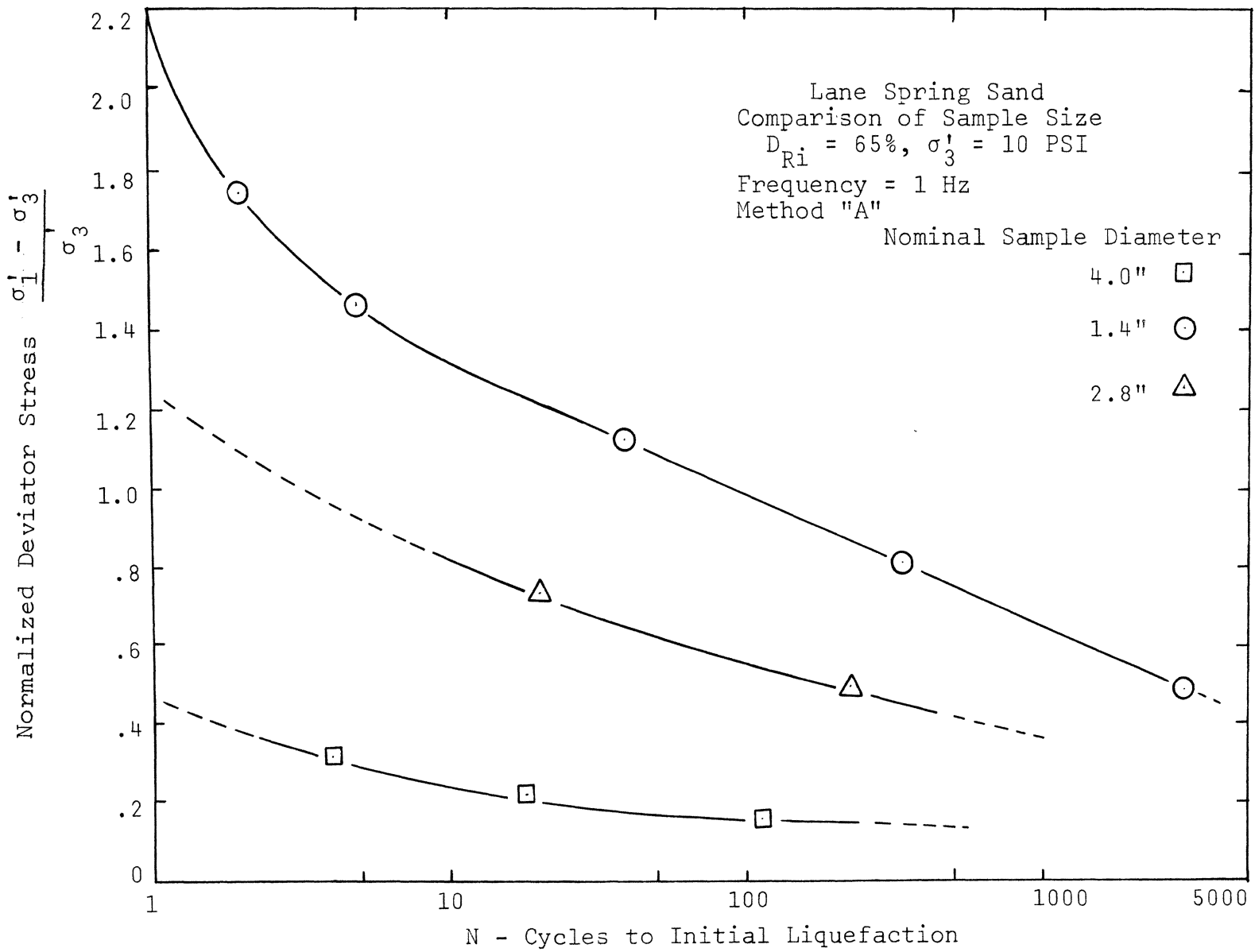
Fig. 5.4 Summary of Test Results of Reversing Stress Tests on Three Sample Sizes.
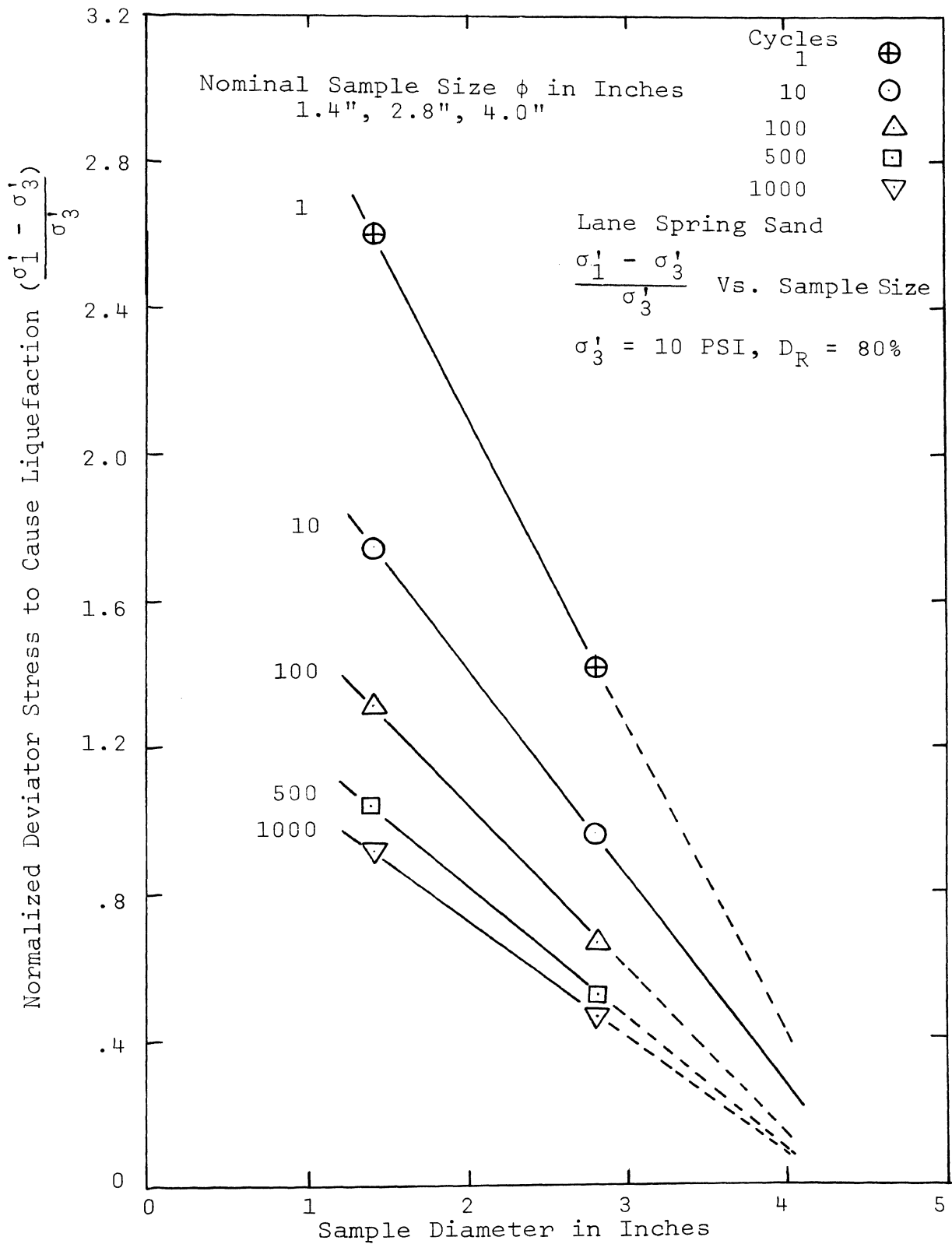
Fig. 5.5 Relationship of Sample Size to Deviator Stress
To Cause Liquefaction (80%)
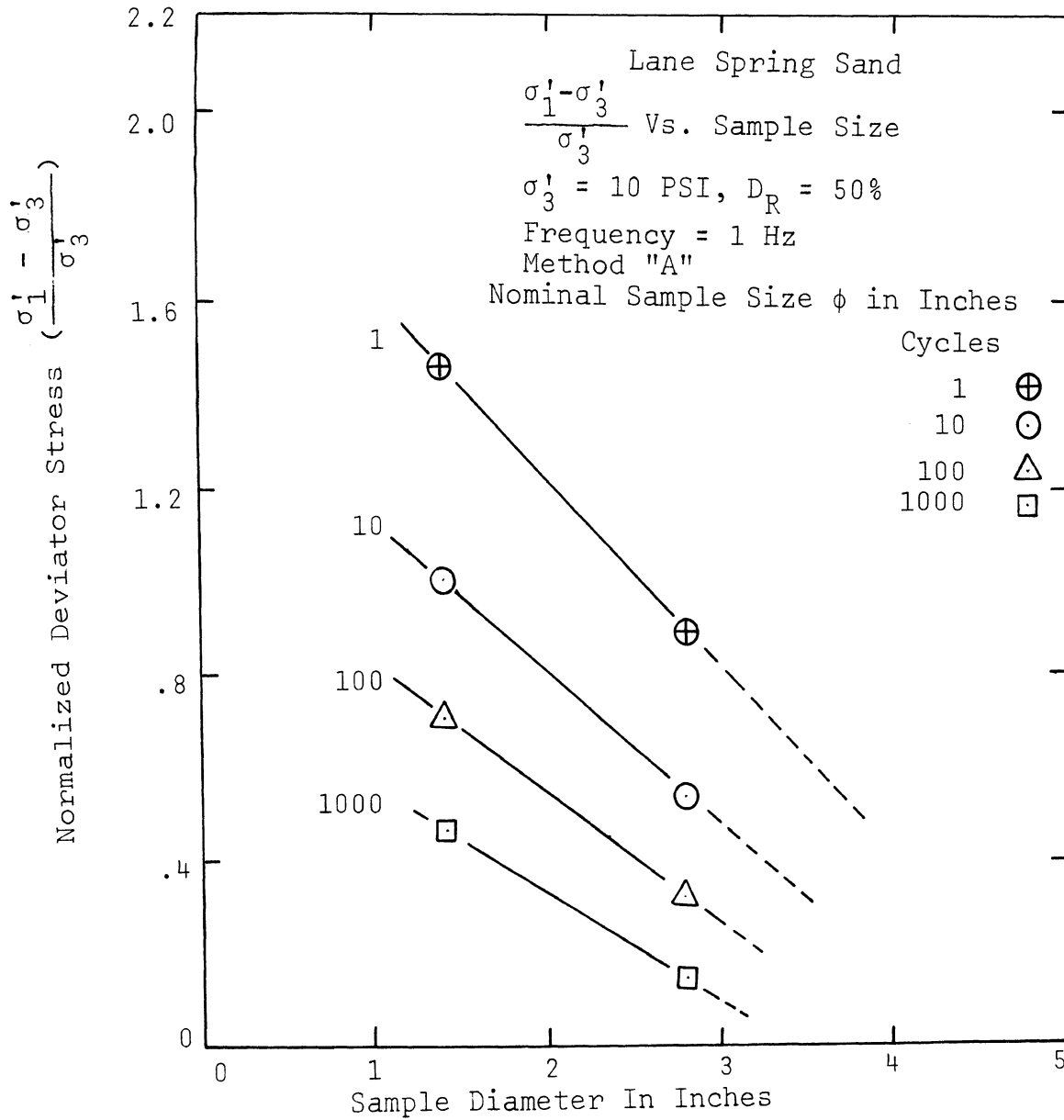
Fig. 5.6 Relationship of Sample Size to Deviator Stress to Cause Liquefaction (50%)
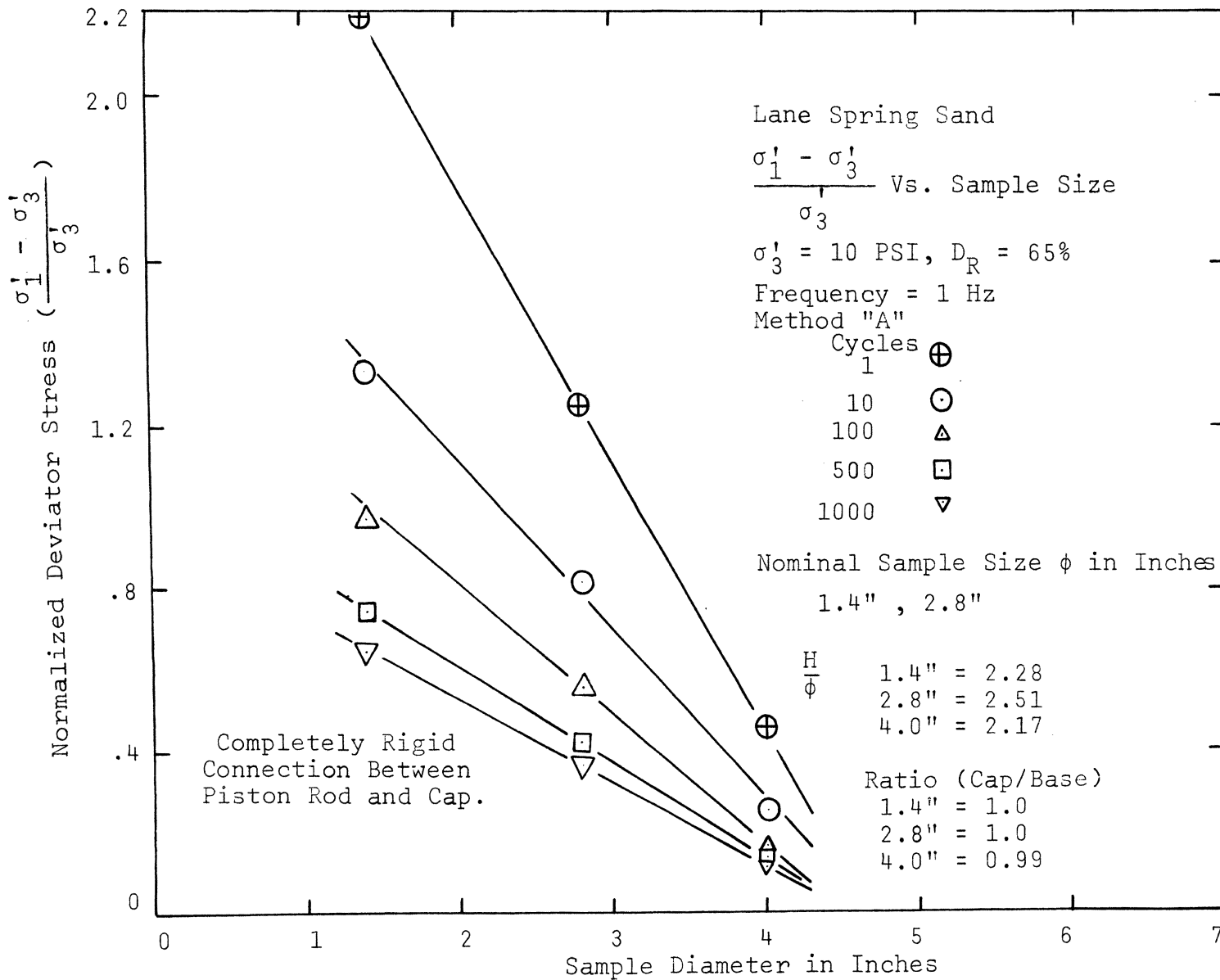
Fig. 5.7 Relationship of Sample Size to Deviator Stress to Cause Liquefaction
(65%)
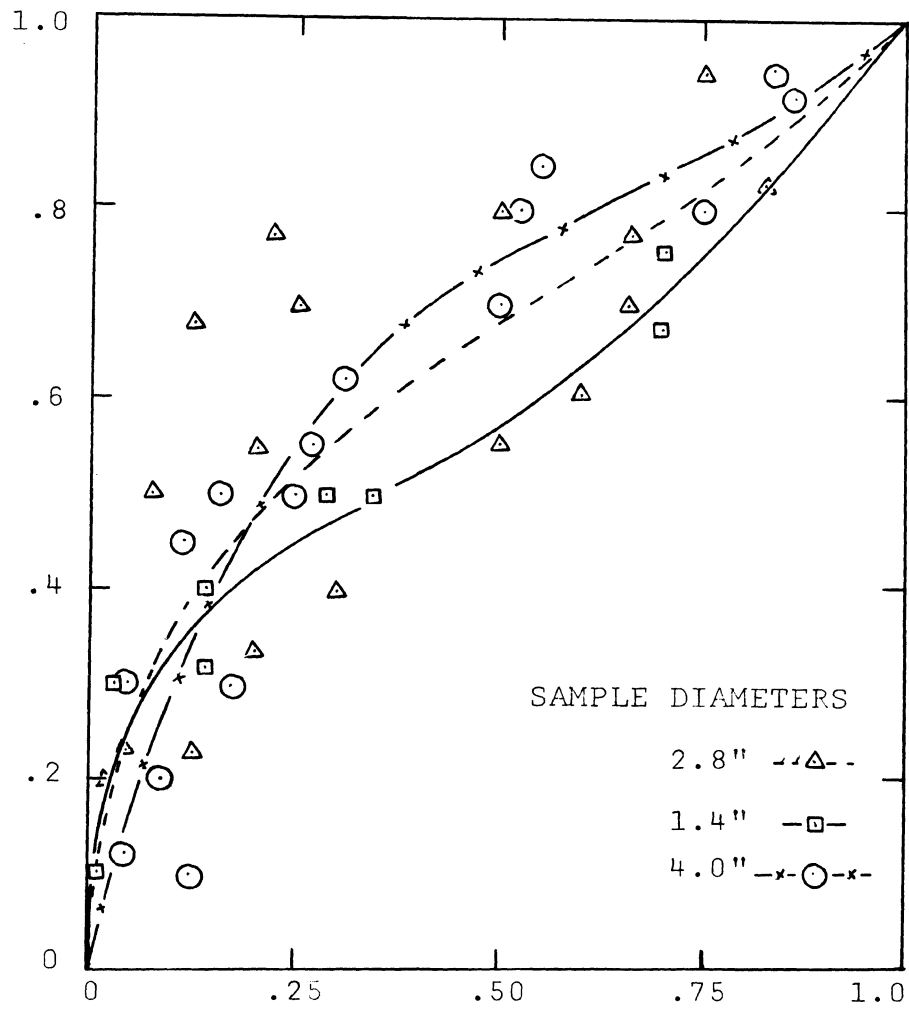
Fig. 5.8   Summary of Pore-Pressure Responses of All the
            Samples in Reversing Stress Tests.
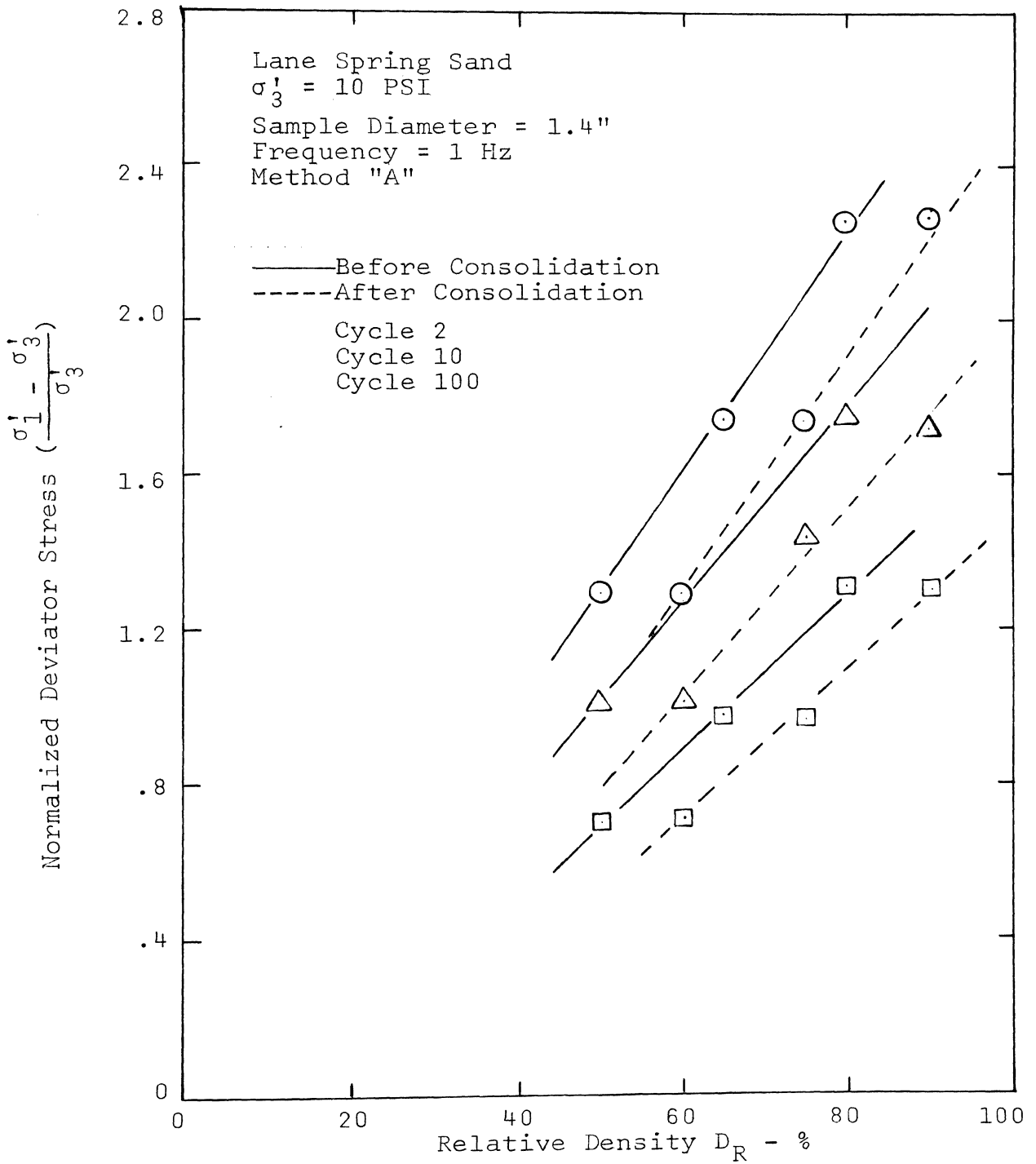
Fig. 5.9 Relationship of Relative Density to Deviator Stress
to Cause Liquefaction
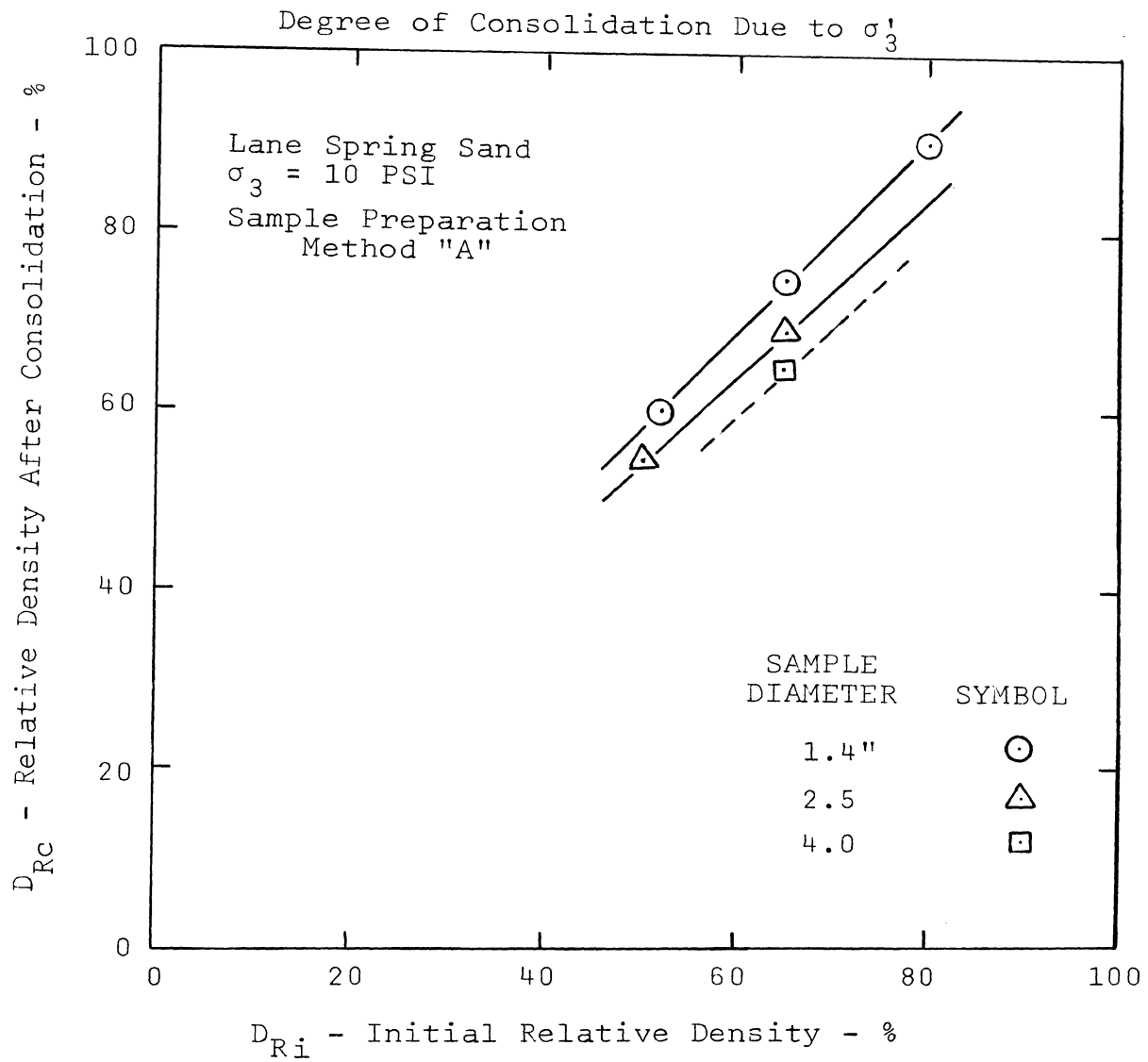
Fig. 5.10   Change in D_R Due to Consolidation
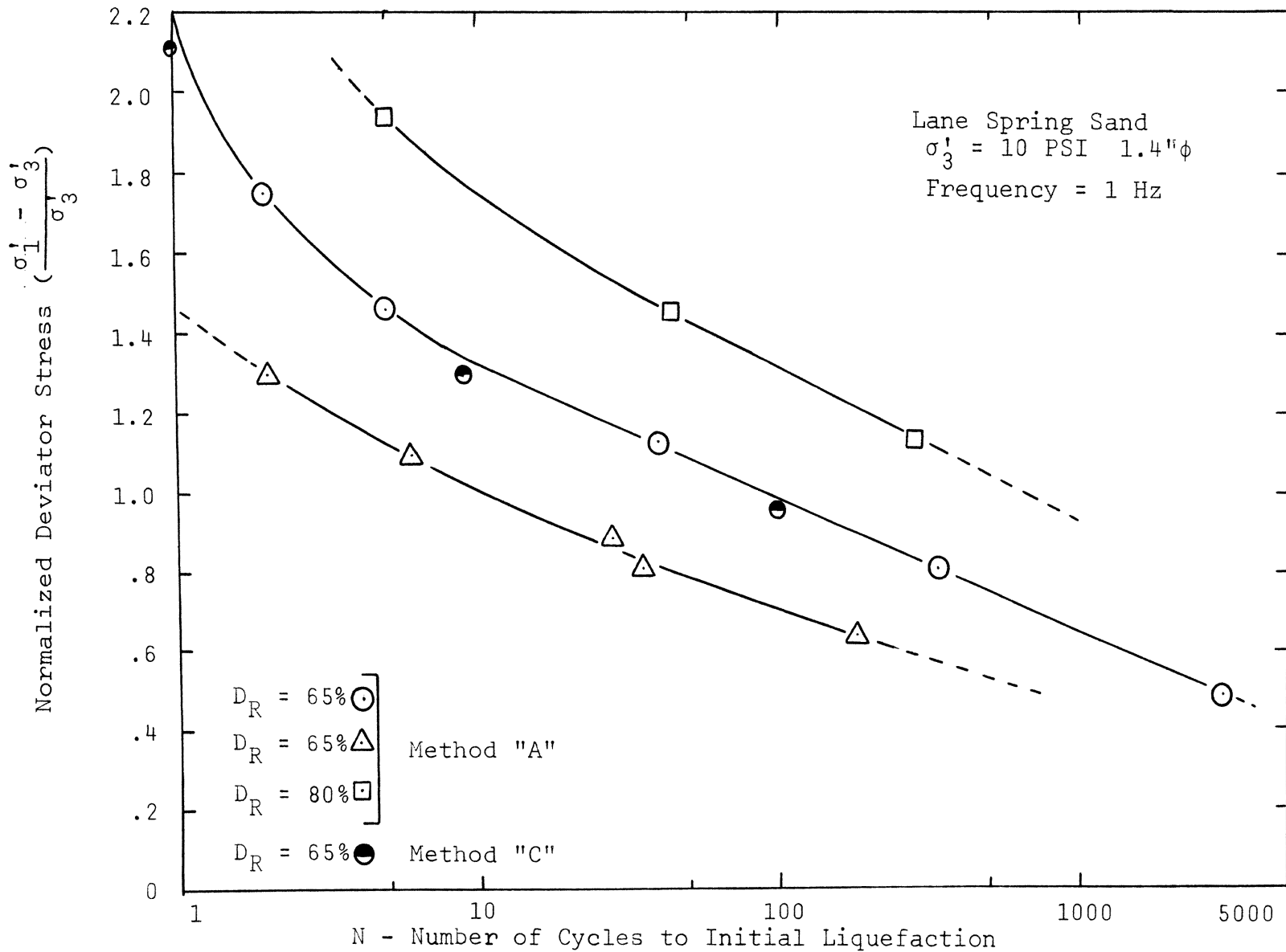
Fig. 5.11 Effects of Sample Preparation Method on the Test Result

The figure plots Normalized Deviator Stress $\left(\dfrac{\sigma_1' - \sigma_3'}{\sigma_3'}\right)$ on the vertical axis versus N — Number of Cycles to Initial Liquefaction on the horizontal axis (log scale from 1 to 5000).

Lane Spring Sand
$\sigma_3' = 10$ PSI $1.4" \phi$
Frequency = 1 Hz

Legend:
$D_R = 65\%$ ⊙
$D_R = 65\%$ △ Method "A"
$D_R = 80\%$ □
$D_R = 65\%$ ● Method "C"

B. Discussion

In this investigation, the majority of the tests were performed on specimens 1.4" in diameter and 3.2" in height prepared by method "A" with an initial relative density of 65%. The results are presented in the middle curve of Figure 5.1, where the normalized deviator stress is plotted versus the number of cycles required to cause initial liquefaction. Initial liquefaction is defined as the state in which the pore water pressure equals the effective confining stress in the sample. It can be seen that as the normalized deviator stress is reduced, a larger number of cycles is required to cause liquefaction. The results are in general agreement with those of Seed and Lee, and Rocker except that the strength of the specimens in this investigation are higher . Previous tests were carried out on three different sands. It is, there-fore, reasonable to expect a variation in strength even under the same conditions and similar test procedures. In this investigation the tests on 1.4" diameter samples with an initial relative density of 65% are referred to as standard tests.

To depict the effects of normalized deviator stress on the number of cycles required to cause liquefaction for different relative densities, test results for relative densities of 50% and 80% are also shown in Figure 5.1. The results follow the same pattern as for the tests at a relative density of 65% and show that the samples with 50%

relative density require fewer cycles to cause liquefaction for a given pulsating deviator stress than soils at a higher relative density. Likewise, samples at 80% initial relative density are stronger than those with 65% relative density.

The data in Figure 5.2 is similar to the middle curve (D_{Ri} = 65%) of Figure 5.1 except that the loading frequency is 2 Hz. In these tests, all other variables are kept constant as in the standard tests. Although the results follow the same pattern as the standard tests, the sample has a lower strength. The curve is almost exactly super-imposed on that of the curve for D_{Ri} = 50% in Figure 5.1. Peacock and Seed have investigated the effects of loading frequency on the strength of sand in cyclic sample shear tests and have concluded that there is no definite pattern in the results; therefore, no definite relationship exists. It cannot be denied that a very limited number of tests have been performed in this investigation and cannot be deemed to be conclusive; a more comprehensive and thorough investigation is required.

The effects on test results due to the variation in specimen sizes are investigated by testing on samples 1.4" in diameter x 3.2" in height, 2.8" in diameter x 6.98" in height, and 4.0" in diameter x 8.5" in height. The test results are presented in Figure 5.3 for 2.8" diameter samples of three different initial relative densities. The trends are similar to those shown in Figure 5.1. The

results on 4.0" diameter samples for D_{Ri} = 65% are shown
on Figure 5.4 along with those for 1.4" and 2.8" diameter
samples under the same conditions. It appears from these
results that a larger sample size gives a lower strength,
i.e. for a given number of cycles, a lower pulsating
deviator stress is required to cause liquefaction for a
4.0" diameter than for a 1.4" or 2.8" diameter sample.
The trend of this result is in agreement with Rocker's [20]
results in a similar investigation on 2.8" diameter samples,
and with Lee and Fitton's [15] observation of the same
phenomenon in their investigation , although all these
investigators attributed the deviation to reasons other
than sample size and none of them investigated this further.
From the present results which is conducted using three
different sample sizes, it clearly appears that a larger
sample gives a lower strength in liquefaction tests, all
other conditions being equal.

Figure 5.4 shows a distinct tendency for the larger
sample to give a lower strength. However, this is not as
startling as it appears to be. As noted by Lee and Fitton,
a larger sample is more likely to have the following
characteristics: 1) discontinuities within the sample;
2) a variation in relative density at different points with-
in the sample; and finally, 3) a variation in grainsize
distribution due to segregation at the time of sample
preparation and vibration for compaction in the mold. The
sample is very likely to exhibit a lower resistance to

liquefaction under repeated loadings.

One possible reason is that a smaller diameter sample appears to consolidate more for the same effective confining pressure than a larger diameter sample. Thus, a smaller specimen may be at a higher relative density at the time of testing than a larger sample, although they are prepared at the same initial relative density.

Another factor in the rapid liquefaction of larger samples is considered to be the quicker pore-pressure response in larger samples. Yoshimi |25| has earlier hypothesized this behavior based on shaking table liquefaction tests on sand. However, it is not clearly understood and reasons behind it could not be completely delineated in this investigation. Data from the previously mentioned figures have been cross plotted to give a relationship between normalized deviator stress and triaxial sample diameter. Figures 5.6 and 5.7 show this relationship for initial relative densities of 50%, 65%, and 80%, respectively. These graphs show that the strength reduction due to larger sample size is more pronounced in tests with high deviator stresses and also at the higher range of relative densities. Perhaps at a higher deviator stress, the first few cycles are more critical as the larger impact on the specimen affects the discontinuities within the sample more severely. The soil structure breaks down producing a local liquefaction which then quickly propagates throughout the specimen. For the given conditions,

Figure 5.8 shows a quicker rise of pore-pressure in larger samples, possibly due to the localized liquefaction because of structure breakdown at the discontinuities in specimen. In any event, there is a greater tendency of volume change in the larger specimens.

Figures 5.9 through 5.11 show the relation of normalized deviator stress relation versus the relative density before and after consolidation of the specimen for samples of 1.4" in diameter. The initial relative density is shown by a solid line for cycles 2, 10, and 100 to cause initial liquefaction. After consolidation, the sample is denser as shown by the dashed-line relationship.

The Figure 5.10 shows an average change in relative densities of the samples of all sizes due to consolidation. It is seen from this graph that the change in relative density for a 1.4" diameter sample is more pronounced than the other two sample sizes. In fact, the change of density in 4" diameter sample is negligible. The 4" diameter sample appears not to consolidate at all.

The effect of sample preparation method is investigated by preparing samples in three different ways. A full description of the methods is given in the Appendix B. The results are reproduced in Figure 5.11. The standard method of sample preparation throughout the investigation is method "A". It is concluded from these tests that the two methods of sample preparation used in the tests do not affect the test results, if required conditions are

achieved in the specimen. The specimen can be prepared in any manner, and if the characteristics of specimen such as initial relative density, diameter, saturation, etc. are substantially the same, it appears this will not have an effect on the test results.

CHAPTER VI

CONCLUSIONS

The effect of relative density, frequency of loading, sample size, and the sample preparation methods on the results of cyclic triaxial tests on saturated sand has been investigated and a relationship established between the number of cycles to initial liquefaction to a given cyclic deviator stress. A test with relative density of 65%, loading frequency of 1 Hz, effective confining stress of 10 PSI, the sample preparation method "A" and the specimen size of 1.4" diameter and 3.2" in height is considered to be a standard test. The choice of these particular conditions for a standard test is guided by some previous investigations. It is considered that a test similar to that used by other investigators would check the performance of the equipment and also would considerably simplify the comparison of results with such investigations. It is reasoned that selecting a standard test whose results could be compared to other investigators would also facilitate comparing the effects of variables studied in this investigation.

For the standard test, the cycles to initial liquefaction for a given cyclic deviator stress is established and all other comparisons are made with these results.

On the basis of observation in this investigation and subsequent discussion in Chapter V, the following conclusions are derived:

1. As the relative density of sand increases, the magnitude of cyclic deviator stress to cause initial liquefaction for a given number of cycles also increases.

2. A larger sample tends to give a lower dynamic strength. That is, for a given cycle, a smaller cyclic deviator stress causes liquefaction in a larger sample.

3. The effect of frequency increase from 1 Hz to 2 Hz appears to reduce cyclic deviator stress to failure for a given cycle; other conditions remaining constant.

4. The cyclic deviator stress to cause liquefaction varies linearly for a given cycle as the sample diameter increases.

5. The pore-pressure response is quicker in larger samples.

6. During consolidation, the relative density changes but σ_{dp}/σ_3' vs D_{Rc} graph remains linear and "translates" to the right.

7. It appears that the 1.4" diameter sample consolidates the most.

8. The method of sample preparation does not effect the result.

APPENDICES

APPENDIX A

NOTATIONS

$\left.\begin{array}{l} A \\ B \\ C \end{array}\right]$ Sample Preparation Methods.

A_c Area of the Loading Cap.

A_R Cross-sectional Area of the Loading Rod.

C_c Coefficient of Curvature.

C_u Coefficient of Uniformity.

D_{Ri} Initial Relative Density.

D_{Rc} Relative Density after Consolidation.

F Load (Force).

F_e Effective Load (Force).

G_s Specific Gravity.

N Stress Cycle.

V_s Volume of Solids.

V_v Volume of voids.

W_{rod} Weight of Loading Rod.

W_s Weight of Solids.

e Void Ratio.

f Frequency of Cyclic Loading.

u Pore-Pressure.

σ Stress.

σ_1 Major Principal Stress.

σ_1' Effective Major Principal Stress.

σ_3 Minor Principal Stress

σ_3'	Effective Minor Principal Stress.
σ_{BP}	Back Pressure.
σ_{3c}	Chamber Pressure.
$\sigma_{3counter}$	Counterbalancing Pressure on Loading Rod.
σ_{dp}	Effective Cyclic Deviator Stress.
ϕ	Sample Diameter.
#	Number.

APPENDIX B

DETAILED DESCRIPTION OF EQUIPMENT

The equipment for this investigation can broadly be divided in three main categories: (i) The triaxial chamber and arrangement for cycling the sample; (ii) The control unit for regulating various test conditions; (iii) The electrical sensors and recorder for recording the test results.

The triaxial chamber is a conventional one, except that the sample plattens are interchangeable for different sizes of sample diameters. The schematic diagram of its base plate is given in Figure 7.1. The chamber is of clear lucite, 6" in diameter and 18" in height, covered with an aluminum top plate which is secured to the base plate by three bolted rods. A Thompson ball busing guides the piston rod. The top plate is provided with a quick connect inlet for application of chamber pressure, and there is another outlet for quick release of pressure from the chamber. There is also a provision for holding the core of LVDT for displacement measurements.

The equipment for cycling the stress in a sample consists of a double action piston with a maximum stroke of 2½" in either direction. The double acting piston is an air tight chamber of 6" diameter and 6" in height. It is divided in the middle by two flexible diaphragms: the lower and upper chamber of the piston have one inlet-outlet
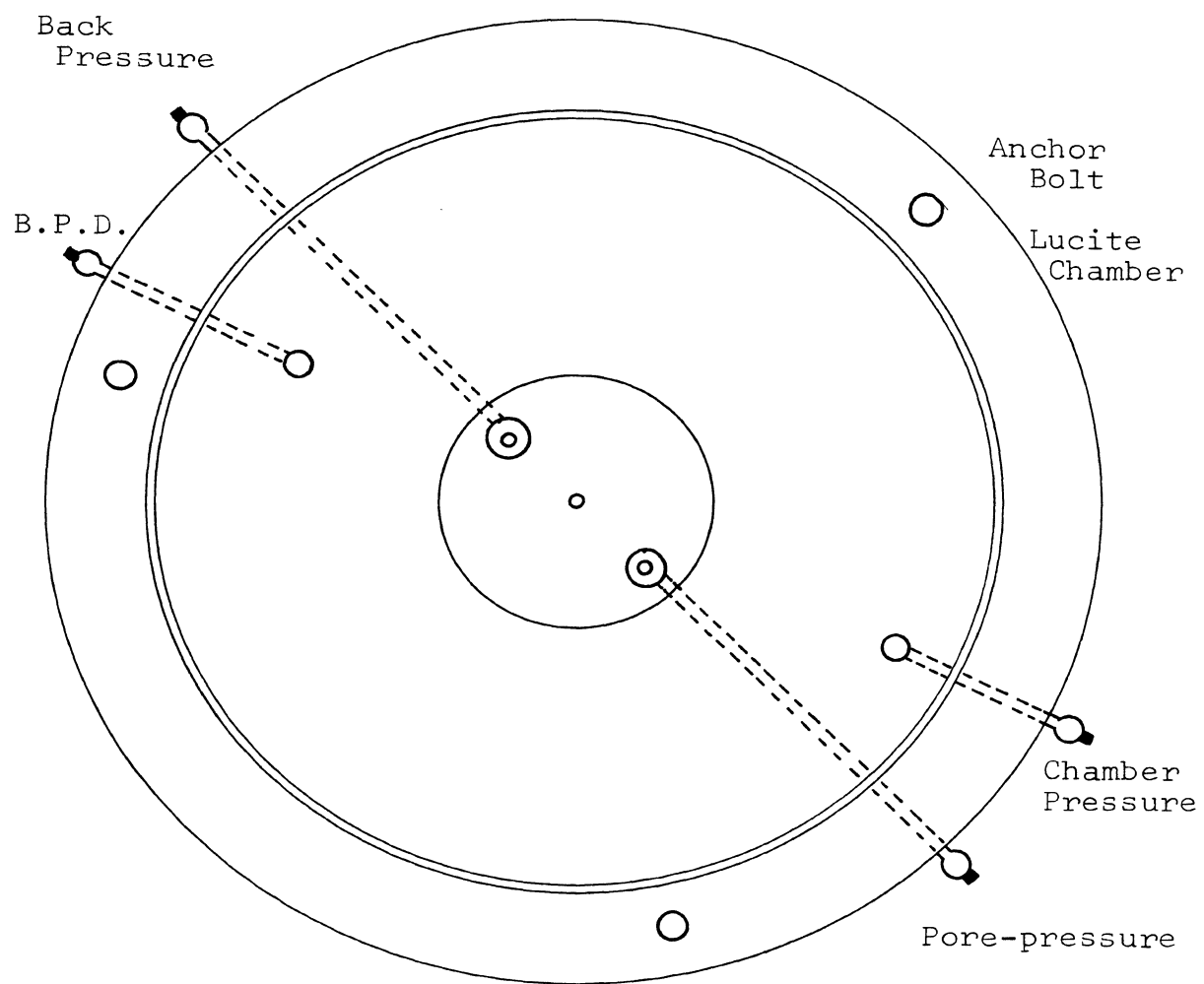
Fig. 7.1 Schematic Diagram of Triaxial Chamber Base Plate

orifice each connecting it to the air supply. The
piston is activated by compressed air, which when filled
in the upper chamber, moves the diaphragms downward and
induces a load in the piston rod in proportion to the air
pressure. When the lower chamber is filled with air, the
diaphragm moves upward to create an extension load in the
piston rod. In this thesis, the downward or compression
load is termed push load and the upward or extension load
is termed pull load. As the piston chambers are provided
with only two orifices, they alternately work as inlets
and outlets. When the upper chamber is connected to
pressure, the lower chamber orifice acts as an exhaust
outlet during downward movement of the diaphragm. Similarly
when the lower chamber is connected to air pressure, the
upper orifice acts as an air outlet for the upper chamber
facilitating the upward movement of the diaphragm. When
the air pressure is cycled into and out of the upper and
lower chambers of the double acting piston, it induces a
downward and upward stroke in the piston rod, consequently
compression and extension stresses respectively are
induced in the sample. The frequency of cycling is con-
trolled by two electrically operated solenoid valves for
upper and lower chamber respectively.

The double acting piston is mounted on a steel frame
directly above the triaxial cell. The triaxial cell is
positioned such that the axies of the piston and triaxial
cell coincide eliminating the possibility of any bending

moment being induced in the loading rod. This reduces error in the recorded load in the sample. The double acting piston rod is connected to the loading rod by a simple nut and screw arrangement, which provides a rigid connection. The arrangement is shown in Figure 7.2.

The control unit for regulating the test conditions such as chamber pressure, deviator stress, loading frequency, etc. consists of one console of electrical and pneumatic systems and four air pressure storage tanks. The schematic diagrams for the pneumatic and electrical systems are given in Figures 4.1 and 4.2.

The pneumatic system consists of one main air pressure inlet, a manifold for air pressure distribution, and six regulators for regulating air pressure, and four air pressure storage tanks. In this investigation only four regulators are used. The regulators for chamber and back pressure are provided by another control panel.

The air pressure in the double acting piston generates a particular stress level in the sample. The four regulator valves control the flow of air into the various pressure regulators. Regulator No. 1 (Push Load) controls the inflow of air in the upper chamber, while Regulator No. 2 (Push Exhaust) controls the exhaust pressure. During the upward stroke, Regulator No. 3 (Pull Exhaust) controls the out-flow and Regulator No. 4 (Pull Load) controls the inflow of air into the piston chamber. Figure 7.4 shows the schematic drawing of the air distribution arrangement.
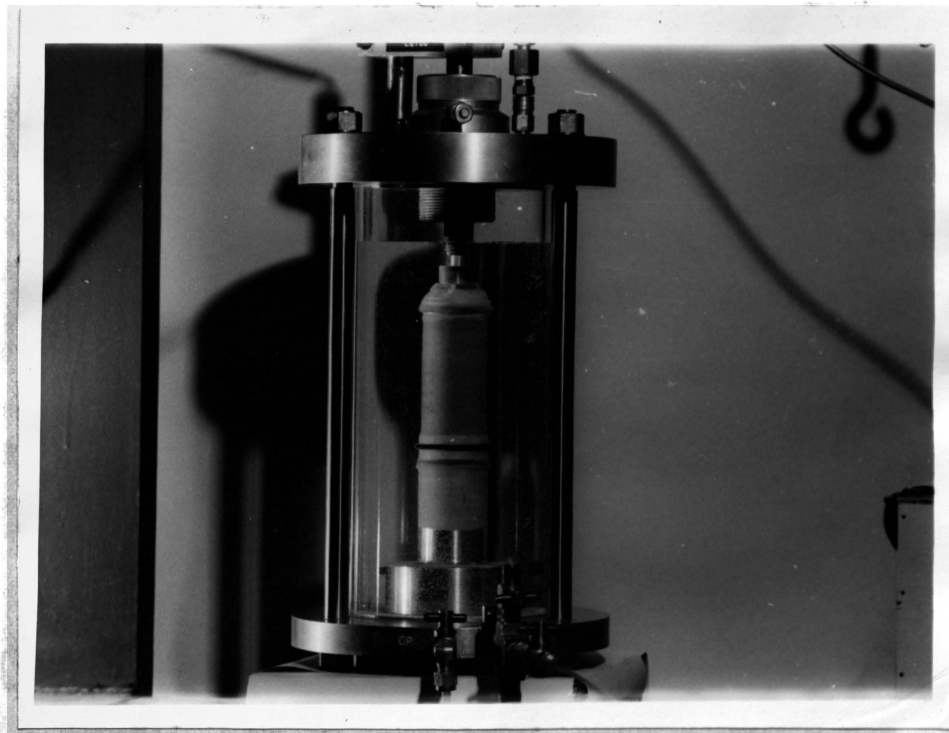
Fig. 7.2 1.4" Diameter Sample
Under Consolidation Pressure

(Note the Nut and Screw Arrangement)
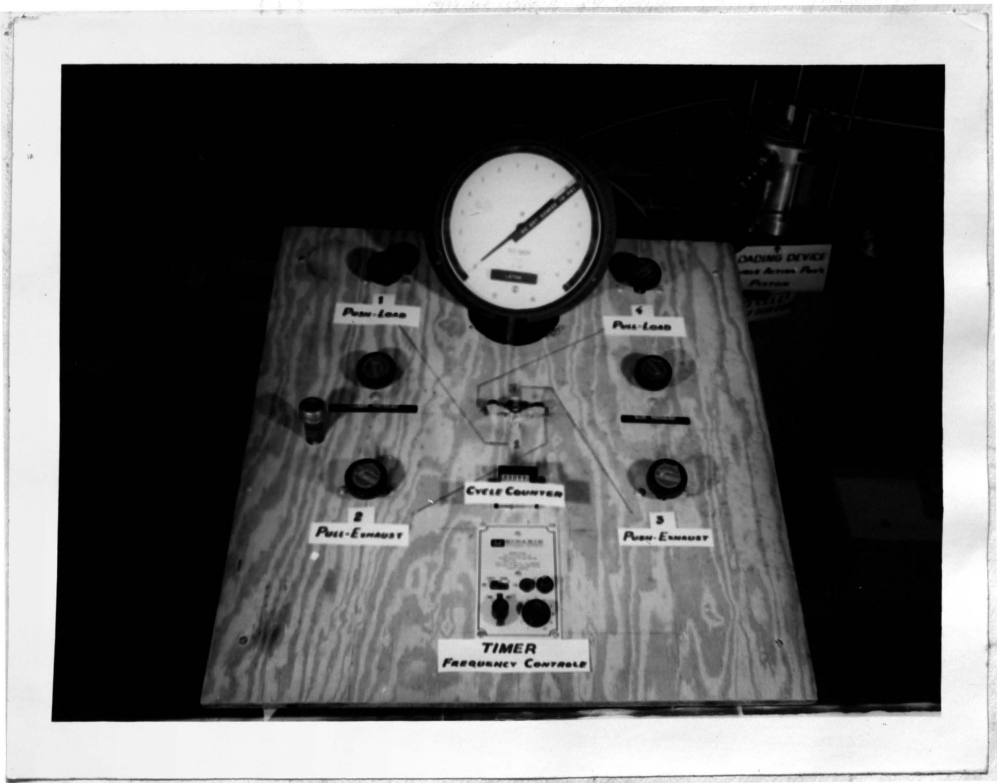
Fig. 7.3   Cyclic Triaxial Control Panel

Cam Position-Small

All Regulators Open,
All tanks with some
air pressure

Tank #1   #2

Tank #4   #3

Tank #1

R1

R4

Tank #4

Tank #2

R2

R3

Tank #3

Air Supply
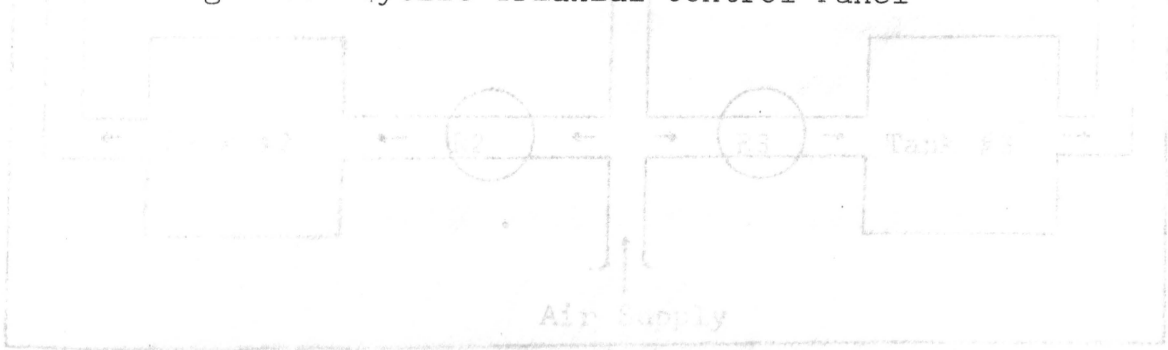
Fig. 7.4   Schematic Diagram of Double Acting Piston

Incoming air is regulated to a pressure gage and a storage
tank. Solenoid valves open and close at the proper time
intervals and provide air to the upper and lower chambers
of the double acting piston. The storage tanks are pro-
vided an air bleeding valve that maintains a constant level
of air pressure in the tank after a pressure is set in
the regulator. This system eliminates pressure fluctuations
in the delivered air. Tubing from the solenoid valve to
the double acting piston is made as short as possible.
This is the only connection for each of the piston chambers.
These connections alternate as a pressure inlet and
exhaust outlet depending on the setting of the solenoid
valves.

To set and determine the magnitude of pressure in the
regulators, only one pressure gauge is provided at the
manifold. It can be connected to any of the four regulators
by turning a Conant four-way valve on the control panel.
Provision of only one gauge has two distinct advantages.
The first is that the pressures are set on one gauge, so
any inherent characteristic of the scale and gauge pre-
cision are the same for all regulators; secondly, it helps
in maintaining a reasonable compactness of the whole panel
which would be affected considerably by addition of three
gauges.

5/8 inch O.D. flexible tubings and brass swagelock
tube fittings are used for all connections. The connection
from the control unit to the double acting piston has a

flow regulator valve on one end of the tubing and a non-displacement Circle Seal valve on the other end. The flow regulator valve regulates the rate of in-flow and out-flow of air to the double acting piston for generating the various kinds of loading wave shapes. The Circle Seal valve provides a means of closing off completely the air flow to the piston when necessary.

The control unit electrical system includes a power receptacle in the back of the console with a master control switch. The main components of the electrical system are a variable speed electrical motor, an electrical switch, two electrically operated solenoid valves, a cycle counter, and a speed control device for the motor.

The motor shaft is connected to a cam which opens and closes an electrical switch activating two solenoid valves. The direction of rotation of the motor is controlled by a switch on the motor control panel. The speed of the motor can be varied by an electrical regulator on the control panel, which in turn, regulates the frequency of the cyclic stress application. The frequency of load application can be varied from 0 Hz to 10 Hz.

The third category of equipment, which is utilized to measure the stresses, deflection and pore pressure inside the sample, consists of one strain gauge load cell, one Hewlett-Packard D.C. Linear Variable Differential Transformer, and one Viatran pressure transducer, together with a Honeywell multichannel light beam oscillograph

(Model 1580 Visicorder) for monitoring the electrical signals from the load cell, LVDT and pore-pressure transducer.

The load cell is mounted between the loading cap of the sample and the double acting piston rod outside the triaxial cell. The load cell has a protruding screw on one end which connects it to the piston shaft, while a threaded groove on the other side receives the loading rod from the sample cap.

The LVDT core is mounted on the top of the triaxial cell and the body is held rigidly by an aluminum clamp attached to the leading rod; therefore, the body of LVDT moves up and down with each stroke of the piston, monitoring the deflection of the sample.

The pore pressure transducer is mounted outside the triaxial cell, approximately 1" below the level of the base plate. It is shown in Figure 4.4 . The transducer is mounted on the lower opening of a solid four-way metal manifold with non-displacement Circle Seal valves mounted on the other three openings. One of the Circle Seal valves is equipped with a Hansen 1800 series Quick connect valve which is used to connect the back pressure device to the sample; the other end is attached to the sample drainage line of the triaxial chamber base plate. The third opening, vertically above the transducer, is used to drain the system.

The specifications and detailed description of the Honeywell oscillograph and the other sensing devices can be found in the technical literature supplied by the manufacturers of these devices.

APPENDIX C

DETAILED PROCEDURE OF SAMPLE PREPARATION

As previously mentioned, the specimens are prepared by three different methods for comparison of their effects on test results. However, there are some general steps which are common to all of the methods, such as: determining the exact amount of sand for a particular relative density; tapping and vibrating the mold for densification; the attaching of the first thin membrane to the base and positioning the mold for sample forming. Each of these steps and the specific technique of the different methods are now described.

To achieve a particular predetermined relative density of the specimen, a calculation is made to obtain the required in place unit weight. The volume of a particular size of sample is determined and weight of sand to fill that volume at minimum void ratio is calculated. Once the weight of sample for minimum void ratio is determined, the weight for any other void ratio can be determined thereafter. A sample calculation for D_{Ri} = 65% is given below as an illustration.

The sample is formed in a thin commercial rubber membrane attached to the bottom platten by a rubber band, carefully placed slightly below the O-ring grooves. The mold is placed around the bottom plate, secured in position by a C clamp. The membrane is then pulled out from the

SAMPLE CALCULATION FOR SPECIMEN WEIGHT

FOR 65% RELATIVE DENSITY

Considering a specimen 1.4" diameter X 3.2" high:

Vol. of specimen $= \pi/4 \ (1.4)^2 \ x \ 3.2 \ in.^3$

$$= 4.928 \ in.^3$$

$$= 80.01 \ cm^3$$

Void Ratio e at 65%

$$e \ = V_v/V_s = 0.571 \ (from \ Figure \qquad)$$

$$or \ V_v = 0.571 \ V_s$$

Vol. of specimen $= 80.01 \ cm^3 = V_v + V_s$

$$or \ 0.571 \ V_s + V_s = 80.01 \ cm^3$$

$$or \ V_s(1+0.571) = 80.01$$

$$or \ V_s = 80.01/1.571 = 50.9 \ cm^3$$

Weight of solids in specimen W_s

$$W_s = G_s \ x \ V_v = 2.64 \ x \ 50.9 = 134.476 \ gms.$$

$$(G_s = 2.64 \ from \ Table \ I)$$

$$= 134.48 \ gms.$$

mold and its free end is rolled onto the neck of the
mold; air trapped between the membrane and the mold wall
is sucked out by application of vacuum, which leaves
no void between the membrane and the mold wall. The
membrane conforms to the exact shape and volume of the
mold. Sometimes the membrane starts slipping off from
the mold neck. In such a case, an O-ring of proper size
is placed over the neck of the mold to keep the membrane
in place. After these steps are complete, the sample form
is ready to receive sand by any of the three methods des-
cribed below.

Method "A" -- In this method, a predetermined amount
of sand for a particular void ratio or relative density is
introduced in a 500 ml. flask. The flask is prefilled
with approximately 250 ml. of warm water. The filled
flask is connected to a vacuum source to de-air the sand
and water in the flask. The flask is agitated continually
to assure the removal of air from every part of the sample.

The triaxial chamber base with mold and membrane is
submerged in a trough of de-aired water. The sand is
introduced into the mold below the water surface. Water
replaced the sand in the flask while the sand flows into
the mold. The sand is never exposed to atmospheric air
at any time during placement. The sand is introduced into
the mold in several layers, depending on the required
relative density. For relative densities of 65% to 70%,
generally three layers are most suitable. Higher densities

require more layers. For a relative density below 50%,
one layer is deposited with very light tapping of the mold
for densification. On the other hand, for higher densities,
more layers, heavy tapping, and sometimes vibrating the
mold may be necessary. When the sand is completely
deposited to a particular height in the mold, to conform
to the predetermined volume, the sample loading cap is
placed on top without disturbing the surface of the sand.
The membrane is carefully rolled over the cap from the
mold neck and a rubber band is slipped around it, again
taking care that the band does not slip into the O-ring
groove. A slight negative pore-pressure is induced inside
the sample, which creates a condition of effective con-
fining stress and prevents the sample from deforming after
the removal from the mold. This is achieved by connecting
the pore-pressure outlet of the base to a vacuum source.
This step creates a condition equivalent to a preconsoli-
dation pressure on the sample. Therefore, the lowest value
of confining pressure was used to prevent sample collapse.

After inducing a negative pore-pressure inside the
sample, the mold is removed and the specimen is left for
one-half to one minute to stand without the mold. The
valve is shut and the vacuum is still maintained. If the
sample does not slump or deform, it is an indication that
the thin membrane enclosing the sample is not leaking or has
not been damaged during the forming of the sample. Never-
theless, to prevent damage to it during the test, a second

Fig. 8.1 Sample Preparation by Method "A"

rubber membrane of 0.01 inch thickness is slipped over the sample by means of a membrane stretcher and sealed on both ends by rubber O-rings sealing the sample. The specimen is then ready for testing after proper assembly of the triaxial cell. The sample is then saturated by back pressure technique.

Method "B" -- After the sample mold is prepared, ready to receive sand as in method "A", sand is introduced in the mold in layers and tapped and/or vibrated to the proper height. The finishing steps are the same as method "A", such as capping, inducing negative pressure, removing the mold, checking for leaks in the membrane and putting another membrane over the sample. The sample is then saturated by the back pressure technique.

Method "C" -- As outlined earlier, this method is very close to method "A". The only variation is that instead of submerging the platten and mold in water and introducing de-aired material, the mold is prefilled with water and dry sand is introduced into the mold in layers maintaining a free water surface on top. After all the finishing steps are taken, the sample is ready for a test of saturation.

In brief, all the steps of specimen preparation can be summarized in a tabular form.

1. Attach a thin membrane to platten by a suitable rubber band.

2. Encase the membrane by forming mold and secure the mold in position.
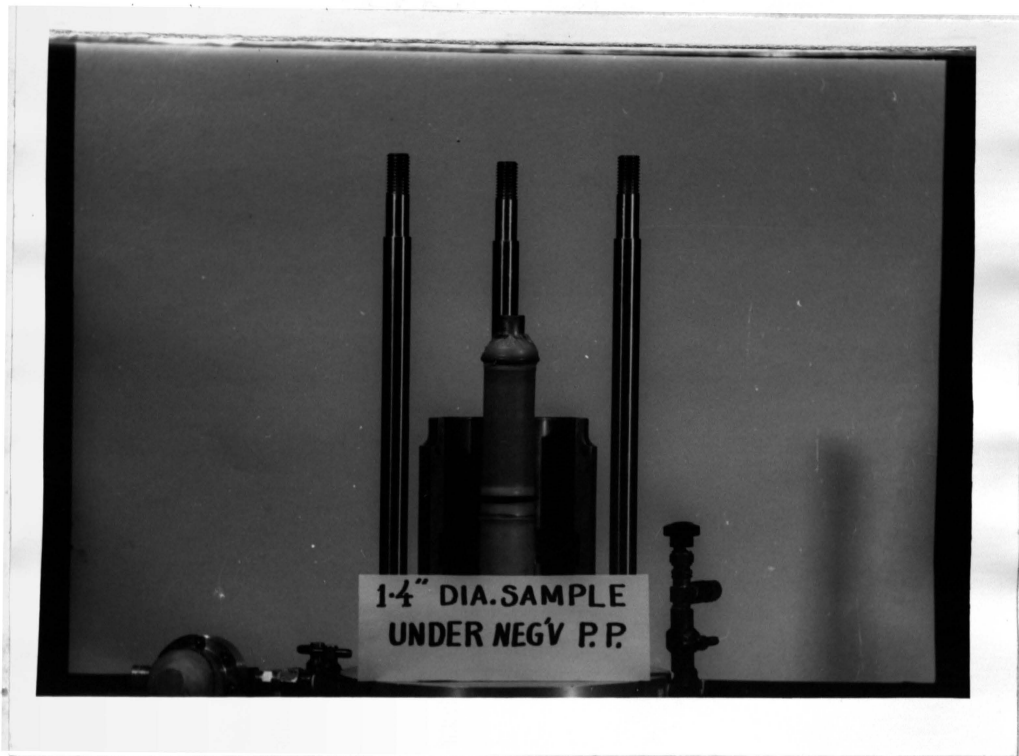
Fig. 8.2 1.4" Diameter Sample Under
Negative Pore-Pressure

3. Take the free end of the membrane out, roll it over the neck of forming mold and secure by an O-ring if necessary.

4. De-air the space between the membrane and mold wall.

5. Introduce sand in the manner desired (submerged, dry or prefilled mold).

6. Place cap on top, unroll the membrane over it and secure by a rubber band.

7. Induce a negative pore pressure inside the sample, close to the preconsolidation pressure desired.

8. Remove the mold and let the sample sit for one-half to one minute to check if the membrane is damaged.

9. Put another membrane over the sample and secure by O-rings on both ends.

After the specimen is formed, the triaxial chamber assembled and proper connections are made to observe the pore-pressure inside the sample, the recorder is activated. A chamber pressure of 10 PSI is applied and the resultant rise in pore-pressure is recorded. From the pore-pressure increase, Skempton's pore-pressure parameter B is calculated. If the value of B is not close to 1.00, a back pressure is applied to the sample, forcing the water in it to bring it to saturation. A pressure differential of 1 PSI is maintained between the chamber pressure and back pressure. The back pressure line is closed and the chamber
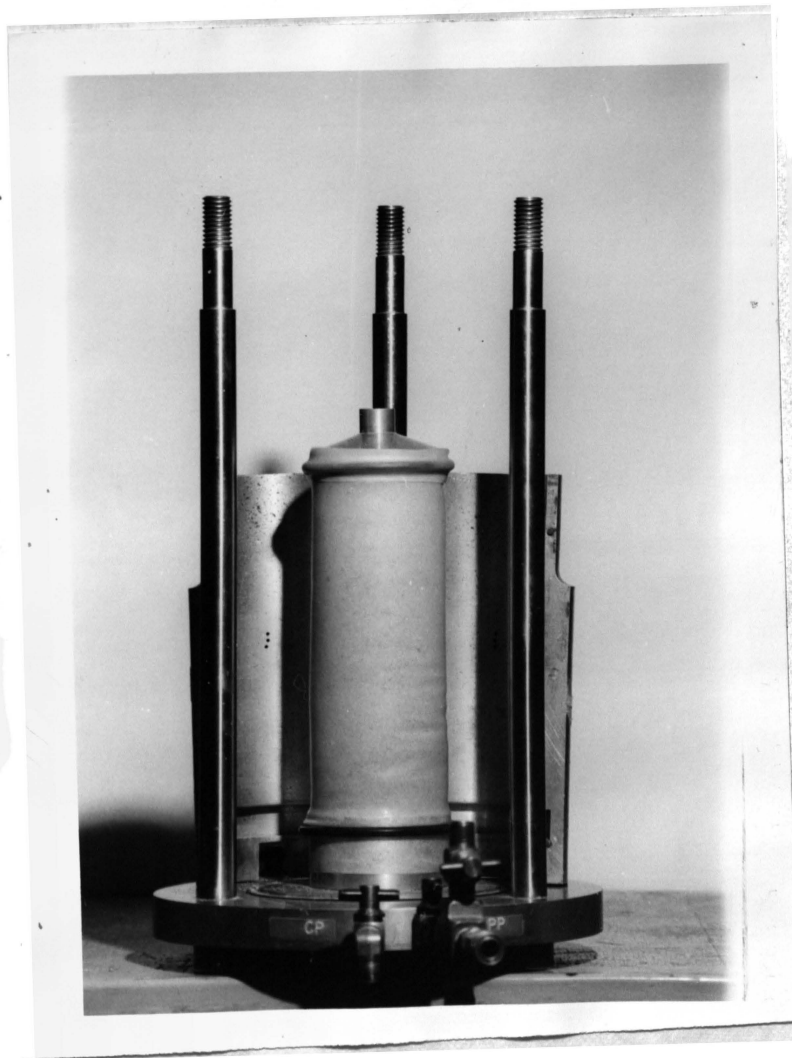
Fig. 8.3   2.8" Diameter Sample Under
Negative Pore-Pressure
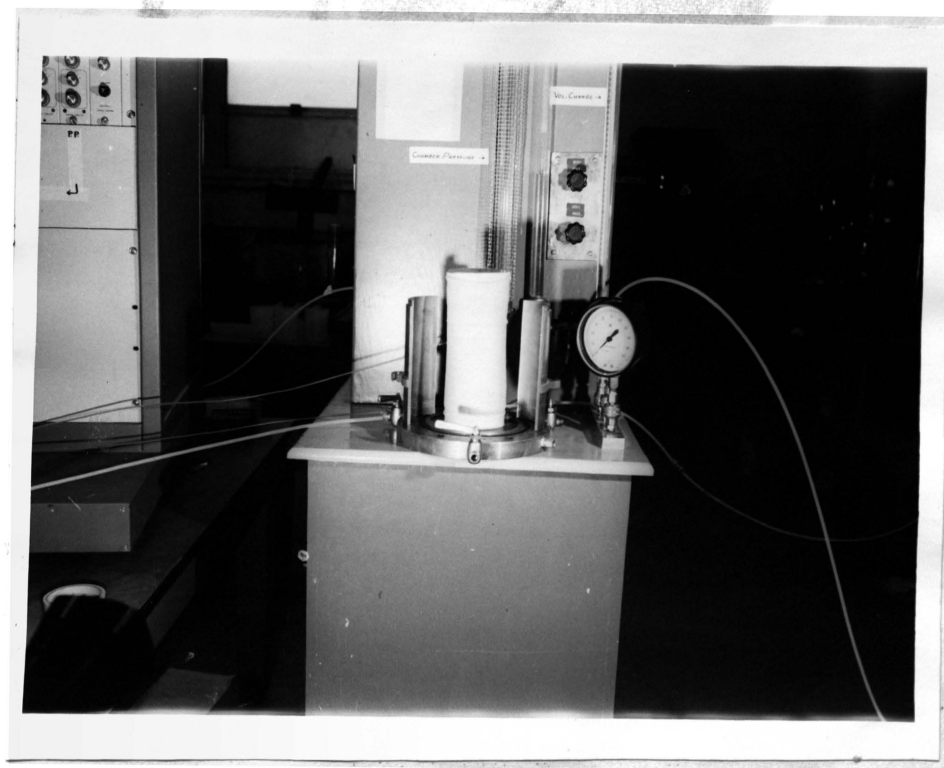
Fig. 8.4 4.0" Diameter
Sample Under Negative Pore-Pressure

pressure again ... and the permanent rise in pore-pressure ... pore-pressure ... This process is ... reaches 1.00 ... at least ... the sample ... considered to behave ... to the desired ... drainage line, which ... is open and the ... r the iso-tropic ...

CYCLIC ...

An ... in a soil element ... quake has been put fo ... to the ... pothes ... of the deform ... of shear waves ... that the soil e ... ains that record ... rthquake, while ... rtant. the cyclic shear stresses ... the element for this duration of the earthquake ... magnitud in the laboratory ... when a cyclic loading ... At the same time, this can also be reproduced approximately in a simple shear condition [23].

Seed and Lee show the three stress conditions at different stages of cyclic triaxial loading test. See

Fig. 8.5 Device for Back Pressure, Chamber
Pressure and Volume Change Measurement

pressure again raised by 10 PSI and the consequent rise in pore-pressure noted for calculation of parameter B. This process is continued in steps until the value of B reaches 1.00 or at least 0.96. When the sample is considered to be saturated, the chamber pressure is increased to the desired level of consolidation stress. The drainage line, which is connected to a volume change burette, is opened and the sample is allowed to consolidate under the iso-tropic confining stress.

CYCLIC ASPECTS OF TESTING

An idealized condition of shear stresses in a soil element below ground surface during an earthquake has been put forward by Seed and Lee |23|. According to the hy-pothesis, during an earthquake, the major portion of the deformations occur due to the upward propagation of shear waves from underlying layers. It is assumed that the soil element is subjected to cyclic shear strains that reverse direction several times during the earthquake, while the normal stress on the plane remains constant. The cyclic shear stresses that are induced in the element for this duration of the earthquake can best be represented in the laboratory by a simple shear test conducted under a cyclic loading condition. At the same time, they can also be reproduced approximately in a triaxial testing condition |23|.

Seed and Lee show the three stress conditions at different stages of cyclic triaxial loading test. See
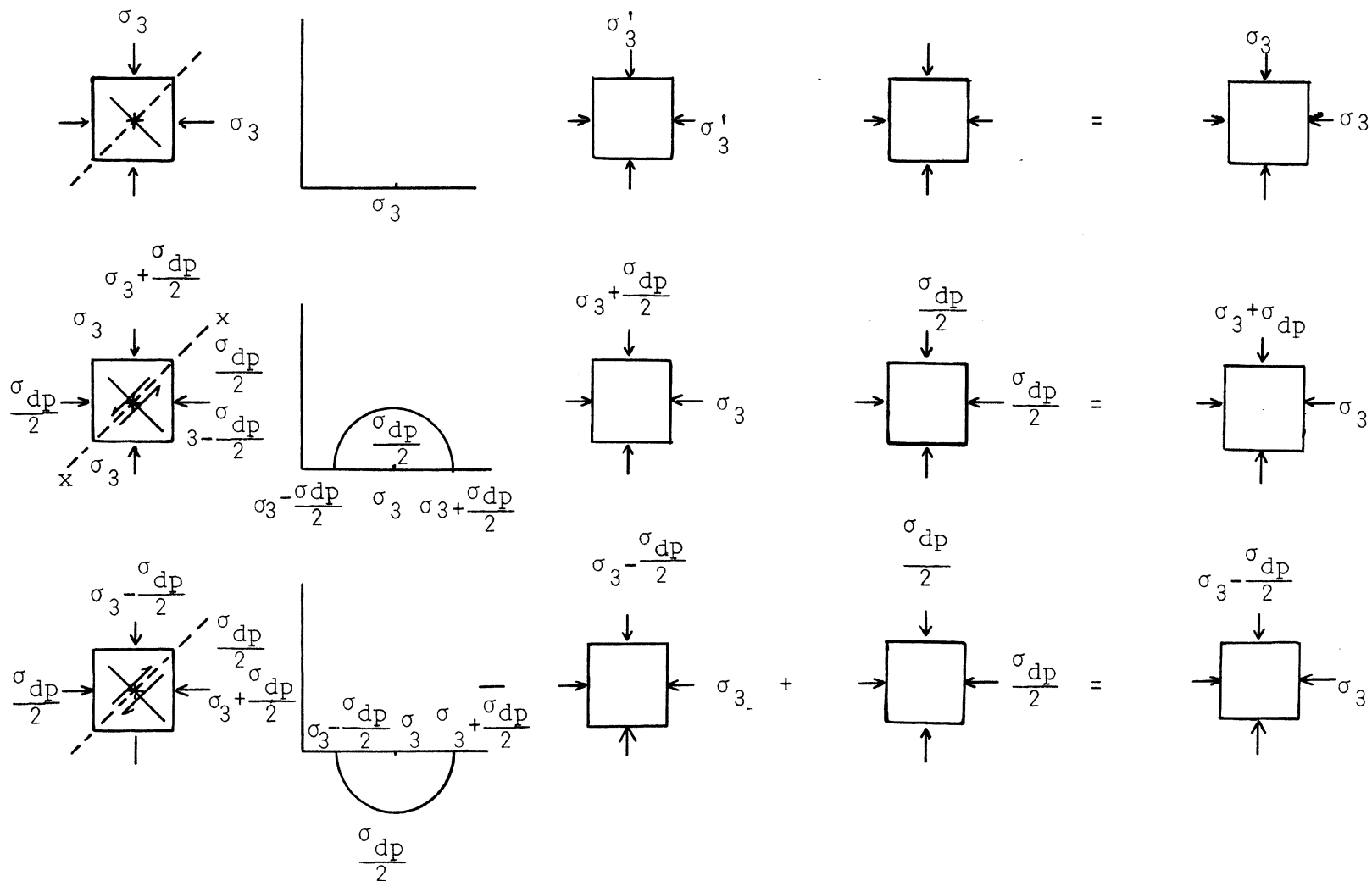
Fig. 8.6 Stress Condition for Triaxial Test on Saturated Sand Under
Simulated Earthquake Condition--After Seed and Lee |23|.

Figure 8.6.

The required cyclic stress changes for inducing the
desired stress condition desired warrants that at all
stages of loading the mean of the major and minor principal
stresses be maintained constant. Furthermore, if the
effects of the intermediate principal stress are neglected,
maintaining this condition would induce the desired stress
condition. This condition is achieved by applying a
deviator stress axially in compression and extension al-
ternately. A full discussion regarding this condition
is given by Seed and Lee |23|.

SETTING PRESSURE IN REGULATORS FOR DEVIATOR STRESS

It has already been explained that in the double
acting piston cylinder arrangement, there are only two
orifices which act as air inlet and outlet alternately;
therefore, at any time if one is connected to the pressure
inlet, the other is connected to the exhaust outlet. Hence,
to understand the complete process of regulating air
pressure in the piston chamber, the following important
characteristics of the equipment must be kept in mind.

    1. For convenience in referring, the regulators
       are designated by a numerical symbol.

           Regulator #1   Push Load

           Regulator #2   Pull Exhaust

           Regulator #3   Push Exhaust

           Regulator #4   Pull Load

2. When there is air in both of the chambers of double-acting piston, the effective air pressure is the pressure difference. Push or Pull (i.e. compression or tension) in nature depends on which one of the pressures is higher in magnitude.

3. When the cam lever is on the smaller cam position, tank #2 (Pull Exhaust) pressure is connected to the upper chamber and tank #4 (Pull Load) is connected to the lower chamber. Similarly, if the larger cam is in position, tank #1 (Push Load) and tank #3 (Push Exhaust) are connected to the upper and lower chambers respectively.

4. The above is true only when the left solenoid valve is in the right side position and the right solenoid valve is in the left side position.

5. At any one time, two pressure tanks are connected to the double acting piston together, that is, tank #1 and #3 and tank #2 and #4. Depending on the position of solenoid valve, these pair of tanks open simultaneously.

6. When there is pressure in all the four tanks, the flow of air to the double acting piston never stops; and at any time, the load in the piston is equal to the difference of pressure in the connected tanks at that moment.

Keeping in mind the above working conditions of this equipment, let us assume that the sample is to be cycled

with a 10 PSI deviator stress (σ_{dp}). The other test
conditions are also given:

σ_{3c} = 80 PSI $\qquad\qquad$ σ_3' = 30 PSI

σ_{BP} = 50 PSI $\qquad\qquad$ cam position = small

When the loading piston is not connected to the sample
loading cap, there is an all round effective stress of 30
PSI on the sample and also an uplift pressure in the loading
rod proportionate to its cross-sectional area due to the
chamber pressure. It, therefore, is necessary to counter
balance the uplift in load in the rod when it is connected
to the sample by downward force in the double acting piston
of equal magnitude. To achieve this, it is imperative
to set a pressure in the upper chamber of the double
acting piston, which would act at all times during the
test. Since tank #1 and #2 are alternately connected to
the upper chamber of the double acting piston, this pres-
sure must be set in these regulators for desired results.
Counter balancing the uplift in the loading rod also
facilitates attaching the rod to the loading cap because
the condition brings the rod in equilibrium, therefore, it
can be brought down to the cap and screwed in exerting a
minimal upward or downward force.

The problem can also be analyzed numerically as
follows:

Given: σ_{3c} = 80 PSI

σ_{BP} = 50 PSI
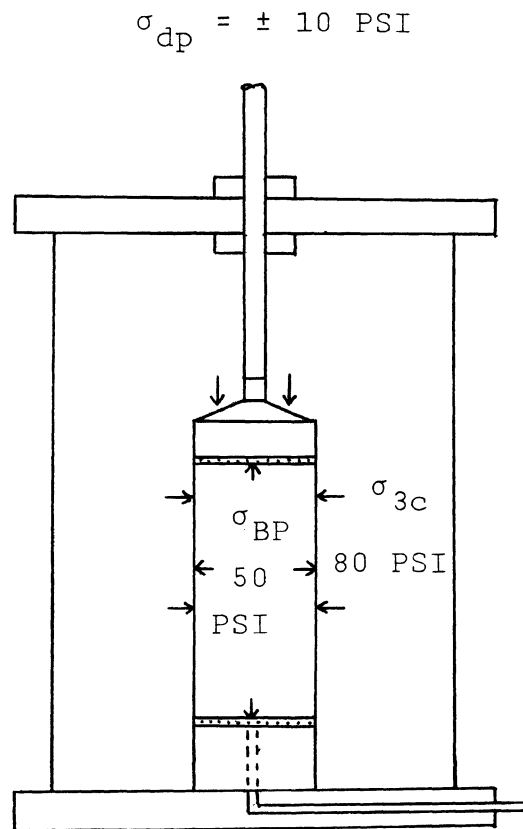
$$\sigma_{dp} = \pm \ 10 \ \text{PSI}$$

Fig. 8.7a   Schematic Condition of Sample
Problem

$$\sigma_3' = 30 \text{ PSI}$$

$$\text{sample } \phi = 1.4"$$

$$\text{wt. of piston rod, load cell LVDT} = 4.5 \text{ lbs.}$$

$$\sigma_{dp} = \pm 10 \text{ PSI}$$

Before the piston is attached, the axial load in the sample:

$$F = (\sigma_{3c} \times A_c) - (\sigma_{BP} \times A_c) = (\sigma_{3c} - \sigma_{BP}) A_c$$

$$= (80 \times 1.54) - (50 \times 1.54) = (80 - 50) \ 1.54$$

$$= 30 \times 1.54 = 46.2 \text{ lbs.}$$

When the loading rod is attached to the top cap, the effective area of the cap exposed to the chamber pressuresure is reduced to an amount equal to the cross-sectional area of the piston rod. The resulting force acting downward on the sample is (for a 1.4" diameter sample):

$$F_e = \sigma_{3c} (A_c - A_R) - (\sigma_{BP} \times A_c) + \text{Wt of Rod}$$

$$F_e = W_{rod} + \sigma_{3c}(A_c) - \sigma_{BP} A_c - \sigma_3 A_p$$

$$= W_{rod} + \sigma_{3c} (A_c - A_p) = \sigma_{BP} A_c$$

$$= 4.5 + 80 \ (1.54 - .442) - 50 \times 1.54$$

$$= 4.5 + 87.8 - 77$$

$$= (87.8 + 4.5 - 77) \text{ lbs.}$$

$$= 15.4 \text{ lbs.}$$

$$\text{Stress on sample} = \frac{F_e}{A_c} = \frac{15.4}{1.54} = 10 \text{ PSI}$$

whereas, the required stress level = 30 PSI or F_e = 46.2 lbs. Therefore, to bring the sample back to an isotropic stress condition, an additional stress of 20 PSI is required and additional air pressure must be induced in the upper

chamber of the double acting piston. This is achieved
by setting a pressure in tanks #1 and #2 such that the
piston exerts an additional 20 PSI on the sample.

For the example problem, the pressure required to
counter balance the piston uplift is calculated as follows:

$$(A_R \times \sigma_{3c}) - \text{Wt of piston rod, LVDT, etc.}$$

$$= (.442 \times 80) - 4.5 = 30.8 \text{ lbs.}$$

Therefore, the required air pressure in the double acting
piston to produce this force is found from a calibration
graph plotted for this purpose; in this case, the pres-
sure required is 1.05 PSI.

Hence the pressure 1.05 PSI is set in the regulators
of tank #1 and #2 for counter balancing the uplift in the
piston rod. When the piston rod is brought to equilibrium
by setting this pressure, it is pulled down to bear against
the sample loading cap and locked in this position by
shutting the Circle Seal valves on the air pressure lines
at the double acting piston. The piston rod can now be
attached to the sample loading cap by screwing it into
the threaded recess of the cap. However, as it is seen
from the first calculations that for the isotropic
conditions in the sample, a force of 46.2 is necessary. A
force of 15.4 is already acting on the sample due to the
chamber pressure in the triaxial cell. The counter
balancing force in the piston rod further provides a force
of 30.8 lbs. on the loading cap that, added to the existing
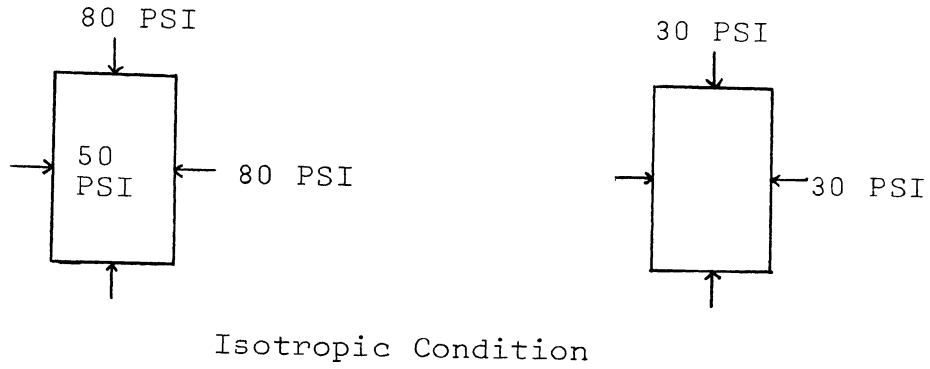
load on the cap results in:

$$(15.4 + 30.8) = 46.2 \text{ lbs};$$

which is necessary for an isotropic stress condition in the sample. The Circle Seal valves on the piston chambers can now be opened, so that the pressure is transferred on the sample.

Once the stress reduction due to the attachment of rod is compensated, the deviator stress can be set in the proper regulators. A schematic analysis is given below for this example condition.

After the stress reduction due to the attachment of the piston rod is compensated, the deviator stress for cycling the sample is set in the proper regulators. At this time, it must be remembered that in the example problem the cam position is "small" at this particular time; this position means that the solenoid valves are open such that tanks #2 and #4 are connected to the upper and lower piston chambers, respectively (see Figure). However, when the test starts, the valves alternately change positions and in the next cycle tank #1 and #3 are connected to the upper and lower chamber of the double acting piston, respectively. This condition requires the test to start with a compressive stroke. The compressive deviator stress must be set in tank #1 and the extension stress in tank #4.

It is, therefore, necessary that in order to exert the deviator stress in the sample, some additional pressure must be set in Regulator #1 and also in tank #4 where there

80 PSI

50
PSI ← 80 PSI

Isotropic Condition

30 PSI

← 30 PSI

$\sigma'_3 - \sigma_{dp} = 30 + 10$

$\sigma'_3 = 30$

Compression

$\sigma'_3 - \sigma_{dp} = 30 - 10$

σ'_3

30

Extension

Desired Condition

Comp.

Ext

Consolidation   Cyclic Str. Reversal   Time
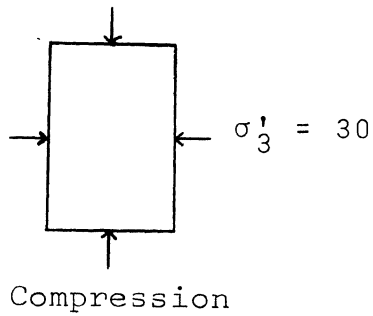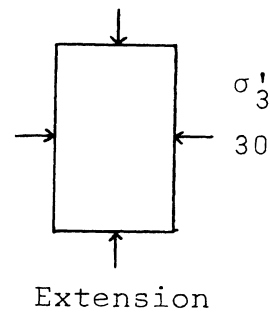
Fig. 8.7b   Schematic Analysis of Sample
Problem

is no pressure at this time. To achieve this, the pressure
for deviator stress that can be determined from the
calibration graph is set in Regulators #1 and #4. On the
other hand, as it is mentioned earlier that tank #4 is
connected to the lower chamber of the piston, any pressure
set in tank #4 will act on the sample due to the upward
movement of the piston, creating an extension stress. To
avoid this condition, the lower chamber of the double
acting piston must be closed by means of the Circle Seal
valve in the air supply line before setting the pressure
in tank #4. The valve is opened only after the test is
started and when the compression stroke is complete. After
this precaution is taken, the pressure can be set in the
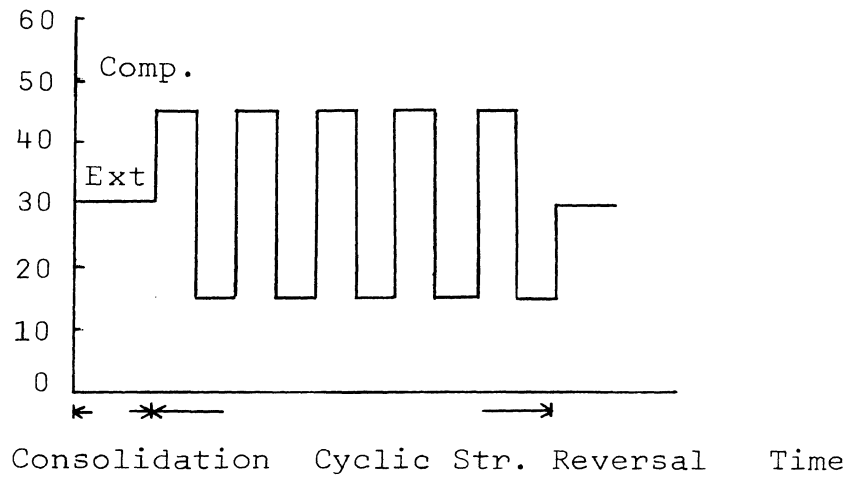regulators for the deviator stress. In the example problem,
a deviator stress of ± 10 PSI is set which is equal to a
force of 15.4 lbs. The corresponding air pressure for this
force is found from the calibration graph, which in this
case is equal to a pressure of 0.85 PSI in the double
acting piston chamber.

Hence, for cycling the sample by a deviator stress of
+10 PSI, a pressure of 0.85 PSI is set in tank #1 for com-
pressive stress over and above the pressure set for
counter balancing the uplift and isotropic condition. A
similar pressure is set in tank #4 for the extension stress.

It follows from the above analysis that after setting
all the pressures in the regulators, the pressure settings

for the example problem will be:

Tank #1 = σ_{dp} + $\sigma_{counter}$ = 0.85 + 1.05 = 1.90 PSI

Tank #2 = $\sigma_{counter}$ = 1.05 PSI

Tank #3 = 0.0

Tank #4 = σ_{dp} = 0.85 PSI

The above procedure for setting the pressure in the regulators as well as running the test is summarized in steps as follows:

STEPS IN PRESSURE SETTING

1. Calculate the uplift force in the piston rod by the equation:

$$A_R \times \sigma_{3c}$$

Subtract the weight of rod, LVDT, load cell, etc. from the calculated force. Balance is the force acting upward on the piston rod.

2. Find the corresponding air pressure to counter balance this force from the calibration graph.

3. Set this pressure in Regulators #1 and #2.

4. Bring the piston rod down to bear against the sample loading cap such as not to exert a pressure on the sample.

5. Lock the piston rod by closing the Circle Seal valves on the air supply lines to the double acting piston.

6. Attach the piston rod to the sample cap by gently screwing it.

7. Set the LVDT on the piston rod.

8. Open the Circle Seal valves on the air supply lines.

9. Find the air pressure required in the piston corresponding to the deviator stress from the calibration graph.

10. Close the valve of lower chamber of the double acting piston.

11. For cam position "small", set this deviator pressure in Regulators #1 and #4. It is possible to set the deviator pressure in the other two regulators; but without complicating the procedure any further, it is always advisable and easier to bring the cam position to "small".

Further steps in continuation for running the test include:

12. Reset the cycle counter to zero.

13. Close the drainage valve beyond the pore-pressure transducer.

14. Start the recorder.

15. Start cycling.

16. Open quickly the lower chamber of the double acting piston as soon as the cam position changes to "large". This occurs in 1/2 cycle.

A note of caution must be added that the calibration graph for laboratory air pressure versus load in the double acting piston and load in piston versus stress in the sample, are two different graphs. Furthermore, a different
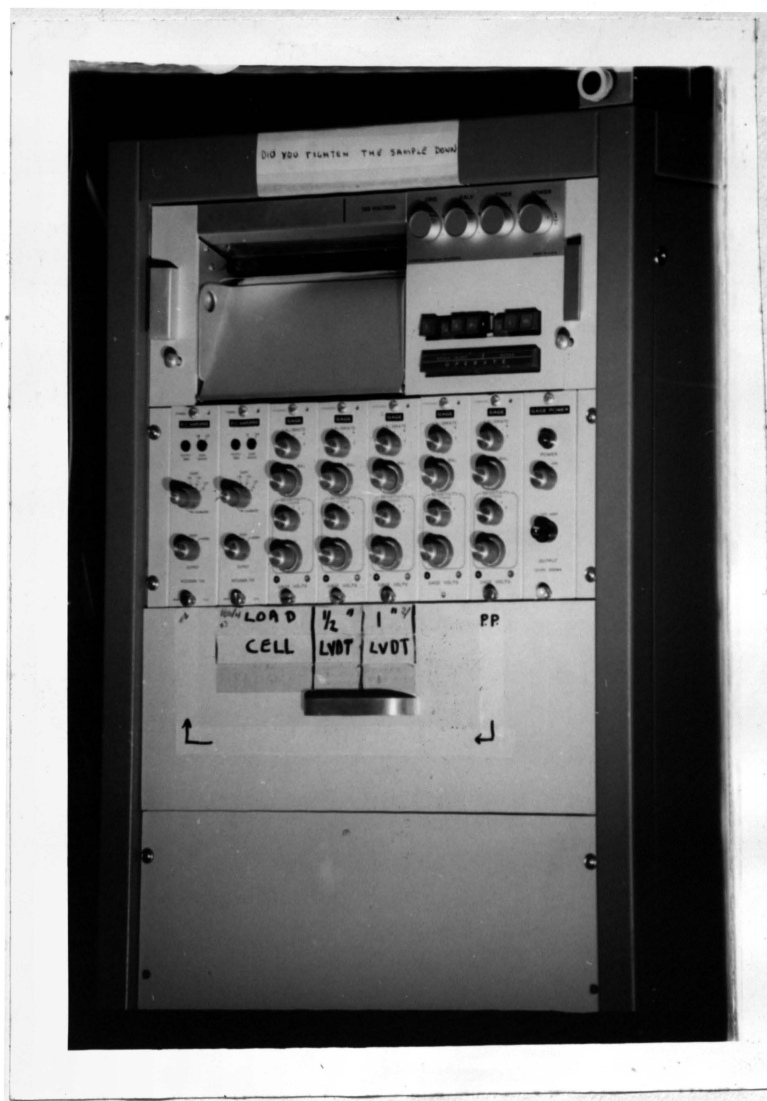
Fig. 8.8   Honeywell Multi-Channel Light
Beam Recorder

calibration graph is required for each different size of sample diameter.

PERFORMANCE OF EQUIPMENT

Performance of the equipment used in this investigation is generally satisfactory. The particular area in which the equipment does not perform well is the calibration of the laboratory air pressure to induce load in the double acting piston. In most cases, the calculated pressure in the regulator did not produce the desired load; invariably the piston generated a smaller loading. This problem is all the more aggravated for loading frequencies of greater value than 1 Hz.

The cause of this behavior is recognized to be the disproportionately large size of the double acting piston. The fluidix of the system is analyzed in a very idealized condition, and this also supports the above observation. Since the double acting piston is an integral part of the equipment system, it is intended to be used for all sizes of samples and ranges of effective confining stresses. However, the piston exerts a force proportional to the area of the piston chamber and a very small magnitude of air pressure, for example 1 PSI, induces a force of more than 28 lbs. in the loading shaft, which amounts to a stress of over 18 PSI in a 1.4" diameter sample. On the other hand, it takes a finite period of time to fill the whole chamber with air before the full pressure can develop. With a

short cycle time, the solenoid setting causes exhaust
before the chamber is completely filled and develops the
intended force.

It, therefore, is recommended that the size of the
double acting piston be kept as small as practicable. A
smaller double acting piston has two advantages. Firstly,
due to its smaller cross-sectional area, it will require
a larger air pressure to generate the same magnitude of
force, thereby increasing the frequency response of the
double acting piston due to a higher rate of in-flow of
air as well as a greater flexibility in the smaller range
of loadings. Secondly, it will reduce the handling diffi-
culty in care of equipment shifting.

The advantage of a large double acting piston is the
flexibility for use with larger size samples.

BIBLIOGRAPHY

1. Bazant, Z. and Dvorak, A. "Effects of Vibrations on
        Sand and Measurement of Dynamic Properties,"
        Proceedings, Sixth International Congress of
        Soil Mechanics and Foundation Engineering, Vol. 1,
        Montreal, 1965, 161-164.

2. Barkan, D.D. Dynamics of Base and Foundations.
        McGraw-Hill, New York, N.Y., 1962, 13.

3. Castro, G. "Liquefaction of Sand," Harvard Soil
        Mechanics Series No. 81. Pierce Hall, Cambridge,
        Mass., January, 1969.

4. Casagrande, A. "Characteristics of Cohesionless Soils
        Affecting the Stability of Slopes and Earthfills,"
        Journal, Boston Society of Civil Engineers,
        January, 1936.

5. Casagrande, A. "The Shearing Resistance of Soils and
        Its Relation to the Stability of Earth Dams,"
        Proceedings, Soils and Foundation Conference of the
        U.S. Engineering Department, June, 1968.

6. Duke, C.M. and Leeds, D.J. "Response of Soils, Foun-
        dations, and Earth Structure to the Chilean
        Earthquake of 1960," Bulletin Seismological Society
        of America, Vol. 62, No. 2, February, 1963.

7. Farrell, R. "A Study of the Behavior of Saturated Sand
        during Repeated Loading." A thesis presented to
        Cornell University for the degree of Master of
        Science

8. Finn, W.D.F., Bransby, P.L., Pickering, D.J. "Effect
        of Strain History on the Liquefaction of Sand,"
        Journal of Soil Mechanics and Foundation Division
        ASCE, Vol. 96, No. SMG, November, 1970, 1917-34.

9. Florin, V.A. and Ivanov, P.L. "Liquefaction of
        Saturated Soil," Proceedings, Fifth International
        Congress of Soil Mechanics and Foundation Engi-
        neering, Vol. 1, Paris, 1961, 107-11.

10. Gullic, R.C. "Multi-Stage Testing of a Cohesionless
        Soil." A thesis presented to the University of
        Missouri-Rolla in partial fulfillment of the
        requirements for the degree of Master of Science
        in Civil Engineering, Rolla, Missouri, 1970.

11. Hardin, B.O. and Black, W. "Vibration Modules of
    Normally Consolidated Clays," Journal of Soil
    Mechanics and Foundation Division, ASCE, Vol. 94,
    No. SMZ, March, 1968, 353-69.

12. Hobbs, W.H. Earthquakes. D. Appleton Co., New York,
    N.Y.

13. Lee, K.L. "Triaxial Compressive Strength of Saturated
    Sand under Seismic Loading Conditions." A thesis
    presented to the University of California,
    Berkeley, California, in partial fulfillment of
    the requirements for the degree of Ph.D. in
    Engineering.

14. Lee, K.L. and Seed, H.B. "Cyclic Stress Conditions
    Causing Liquefaction of Sand," Journal of
    Soil Mechanics and Foundation Division, ASCE,
    Vol. 93, No. SMI, January, 1967, 47-70.

15. Lee, K.L. and Fitton, J.A. "Factors Affecting the
    Cyclic Loading Strength of Soil," Vibration
    Effects of Earthquakes on Soils and Foundations,
    ASTM STP 450, American Society for Testing
    Materials, 1969.

16. Maslov, N.N. "Questions of Seismic Stability of Sub-
    merged Sandy Foundations and Structures," Pro-
    ceedings, Fourth International Conference on
    Soil Mechanics and Foundation Engineering, London,
    England, 1957.

17. "Niigata Earthquake of 1960," Japan National Committee
    on Earthquake Engineering, Third World Conference
    on Earthquake Engineering, February, 1965.

18. Nunnally, S.W. "Development of a Liquefaction Index
    for Cohesionless Soils." A thesis presented to
    the Northwestern University in partial fulfillment
    of the requirements for the degree of Ph.D.,
    Evanston, Illinois, 1966.

19. Peacock, W.H. and Seed, H.B. "Sand Liquefaction Under
    Cyclic Loading Simple Shear Conditions," Journal
    of the Soil Mechanics and Foundations Division,
    ASCE, Vol. 94, No. SM 3, May, 1968.

19.1 Prakash, S. and Mathur, J.N. "Liquefaction of Fine
    Sand under Dynamic Load," Proceedings, Fifth
    Symposium of the Civil and Hydraulic Engineering,
    Indian Institute of Science, Banglore, India, 1965.

20. Rocker, C. Jr. "Liquefaction Behavior of Sand Subjected to Cyclic Loading," Massachussetts Institute of Technology Research Report R68-36, Soil publication No. 221, Cambridge, Massachussetts, 1968.

21. Roscoe, K.H. "An Apparatus for the Application of Simple Shear to Soil Samples," Proceedings, Third International Conference on Soil Mechanics and Foundation Engineering, Vol. 1, Zurich, 1953, 180-91.

22. Roscoe, K.H. and Schofield, A.N. "On the Yielding of Soils," Geotechnique, Vol. 7, 1958, 25-53.

23. Seed, H.B. and Lee, K.L. "Liquefaction of Saturated Sands during Cyclic Loading," Journal of Soil Mechanics and Foundation Engineering Division, ASCE, Vol. 92, SM6, November, 1966, 105-34.

24. Watson, J.D. "Stress Development Characteristics of Cohesionless Soil from Triaxial Tests." A thesis presented to Harvard University for the degree of Sc.D., Cambridge, Massachussetts, 1940.

25. Yoshimi, Y. "Discussion on Liquefaction of Saturated Sands during Cyclic Loading," Journal of Soil Mechanics and Foundation Engineering Division ASCE, Vol. 93, SM5, September, 1967, 327-28.

VITA

Suresh Kumar Chaudhary, son of M.P. Chaudhary and Tarkeshwari Chaudhary, was born on July 19, 1941, in Hazaribagh, Bihar, India. He received his primary and secondary education in the cities of Hazaribagh and Muzaffarpur. After completing the first two years of college at L.S. College of the University of Bihar, Muzaffarpur, he entered Tirhut School of Engineering in September, 1960, at Muzaffurpur, Bihar, India. Upon graduation in May, 1964, he was employed as an engineer in the Department of Minor Irrigation of the Government of Bihar; and then in the Aviation wing of the Public Works Department of the Government of India. In 1967, he emmigrated to the U.S.A. and worked for Law Engineering Testing Co. in Atlanta, Georgia, and Birmingham, Alabama, as a laboratory engineer. He entered the University of Missouri-Rolla in January, 1969, and received a B.S.C.E. in January, 1970.

He has been enrolled in the Graduate School of the University of Missouri-Rolla since January, 1970.